

Jürgen Alexander Waxenegger

# **Imaging excitons in carbon nanotubes with plasmonic nanoparticles**

Diplomarbeit

zur Erlangung des akademischen Grades eines  
Magisters  
an der Naturwissenschaften Fakultät der  
der Karl-Franzens-Universität Graz

Betreuer: Ao. Univ. Prof. Mag. Dr. Ulrich Hohenester

Institut für Physik  
Fachbereich Theoretische Physik  
Karl-Franzens-Universität Graz

2010



# Contents

<b>1</b>	<b>Introduction</b>	<b>3</b>
<b>2</b>	<b>Plasmonic nanoparticles</b>	<b>5</b>
2.1	Metallic nanoparticles . . . . .	5
2.1.1	Dielectric function . . . . .	6
2.1.2	Volume plasmons . . . . .	8
2.1.3	Jellium model . . . . .	8
2.2	Particle plasmons . . . . .	12
2.2.1	Surface plasmon polaritons . . . . .	12
2.2.2	Particle plasmons . . . . .	17
2.3	Boundary element method . . . . .	22
2.4	Plasmon dynamics . . . . .	27
2.5	Electric dipole interactions . . . . .	29
<b>3</b>	<b>Carbon nanotubes</b>	<b>35</b>
3.1	Carbon nanotubes . . . . .	36
3.1.1	Electronic structure of graphene . . . . .	36
3.1.2	Electronic structure of carbon nanotubes . . . . .	40
3.1.3	Electric dipole vector of carbon nanotubes . . . . .	44
<b>4</b>	<b>Imaging excitons in carbon nanotubes with plasmonic nanoparticles</b>	<b>51</b>
4.1	Excitons . . . . .	51
4.1.1	Elementary excitations . . . . .	52
4.1.2	The interband polarization . . . . .	52

4.2	The interband polarization for carbon nanotubes . . . . .	57
<b>5</b>	<b>Conclusion</b>	<b>63</b>

# Kurzfassung / Abstract

## **Abbildung von Exzitonen in Kohlenstoffnanoröhren mit plasmonischen Nanoteilchen**

In dieser Arbeit untersuchen wir die Abbildung von Exzitonen in Kohlenstoffnanoröhren mit plasmonischen Nanoteilchen. Zur Beschreibung der Partikelplasmonen wird die Randelementmethode verwendet. Die Interband-Polarisation der Kohlenstoffnanoröhre wird mit dem Formalismus der zweiten Quantisierung berechnet. Bei der Berechnung des Dipolmatrixelements in paralleler und normaler Richtung wird die Tight-Binding-Methode verwendet. Die Wechselwirkung wird für unterschiedliche Positionen des metallischen Nanoteilchens bezüglich der Nanoröhre untersucht.

## **Imaging excitons in carbon nanotubes with plasmonic nanoparticles**

In this thesis we study the imaging of excitons in carbon nanotubes with plasmonic nanoparticles. For the description of the particle plasmons the boundary element approach is used. The interband polarization of the carbon nanotube is found with the formalism of second quantization. For the calculation of the parallel and perpendicular dipole matrix element a tight binding model is used. We study the interaction for different positions of the metallic nanoparticle relative to the nanotube.



# Chapter 1

## Introduction

Nano-optics studies optical phenomena on the nanometer scale which is near or beyond the diffraction limit of light [NH06]. An important constituent of nano-optics is plasmonics, which is based on interaction processes between electromagnetic radiation and conduction electrons at metallic interfaces or in small metallic nanostructures. The local excitations on metallic nanoparticles are called particle plasmons or local surface plasmon resonances. Their properties depend on the interparticle coupling [Trü07], [HT08a], [HT08b], [HK05] and on the dielectric constant of the environment [Fis88], and they can be used as a sensing element [Sqa02] [Kal01] [Boy02]. Interesting applications are also given by studying the coupling of plasmons to excitons [Tor09] [ZG06]. Semiconducting single-walled carbon nanotubes are promising tools for nanoelectronics. One way of imaging excitons in single-walled carbon nanotubes [Har05] is with plasmonic nanoparticles.



## Chapter 2

# Plasmonic nanoparticles



Figure 2.1: This picture shows the Lycurgus cup at the British Museum in London. When illuminated from outside it appears green. However, when illuminated from within, it glows red. The glass contains metal nanoparticles, gold and silver, which give it these unusual optical properties. source: nanowerk.com

### 2.1 Metallic nanoparticles

Nanoparticles have a size of about 10 to 100 nanometers in each spatial direction. Nanoparticles exhibit size-related properties that differ from those

of bulk materials. One example is the existence of surface plasmons confined to metallic nanoparticles. One possible method to create them is the use of electron beam lithography. We refer to [Aus06] .

### 2.1.1 Dielectric function

A dielectric function describes how an electric field affects a polarizable medium. Over a wide range the optical properties of metals can be explained by the plasma model. It can also be extended to conducting materials. The following definitions and calculations are based on [NH06] and [Mai07].

#### Plasma model

In the plasma model, a gas of free electrons moves against a fixed background of positive ions. The equation of motion for an electron under the influence of an external electromagnetic field is

$$m\ddot{\vec{x}} + m\gamma\dot{\vec{x}} = -e\vec{E}. \quad (2.1)$$

Here  $\gamma = 1/\tau$  is the characteristic collision frequency and  $\tau$  is the relaxation time of the free electron gas. By making an ansatz of a harmonic driving field with frequency  $\omega$

$$\vec{E}(t) = \vec{E}_0 e^{-i\omega t} \quad (2.2)$$

we find:

$$\vec{x}(t) = \frac{e}{m(\omega^2 + i\omega\gamma)} \vec{E}(t). \quad (2.3)$$

The macroscopic polarization

$$\vec{P} = -ne\vec{x} \quad (2.4)$$

by the displaced electrons then becomes

$$\vec{P} = -\frac{ne^2}{m(\omega^2 + i\omega\gamma)} \vec{E}. \quad (2.5)$$

For the dielectric displacement

$$\vec{D} = \epsilon_0 \vec{E} + \vec{P}, \quad (2.6)$$

we get:

$$\vec{D} = \epsilon_0 \left(1 - \frac{\omega_p^2}{\omega^2 + i\omega\gamma}\right) \vec{E}. \quad (2.7)$$

Here

$$\omega_p^2 = \frac{ne^2}{\epsilon_0 m} \quad (2.8)$$

is the the square of the plasma frequency. The complex dielectric function of the free electron gas is therefore given by

$$\epsilon(\omega) = 1 - \frac{\omega_p^2}{\omega^2 + i\omega\gamma}. \quad (2.9)$$

Its real and imaginary parts are

$$\epsilon'(\omega) = 1 - \frac{\omega_p^2 \tau^2}{1 + \omega^2 \tau^2} \quad (2.10)$$

$$\epsilon''(\omega) = \frac{\omega_p^2 \tau}{\omega(1 + \omega^2 \tau^2)}. \quad (2.11)$$

The dielectric function of the plasma model can also be linked to the conductivity  $\sigma(\omega)$ :

$$\epsilon(\omega) = 1 + \frac{i\sigma(\omega)}{\epsilon_0 \omega}. \quad (2.12)$$

Therefore this is also known as the Drude model of the optical response of metals. It describes the optical response of metals only good for photon energies below the threshold of interband transitions. However a description of the optical properties of gold and silver at visible frequencies can be found by describing the interband transitions with the classical picture of a bound electron with resonance frequency  $\omega_0$

$$m\ddot{\vec{x}} + m\gamma\dot{\vec{x}} + m\omega_0^2\vec{x} = -e\vec{E}. \quad (2.13)$$

### 2.1.2 Volume plasmons

The physical meaning of  $\omega_p$  can be understood by looking at the collective longitudinal oscillations of the conduction electrons against the fixed positive background. The displacement by a distance  $u$  generates a charge density

$$\sigma = \pm ne u. \quad (2.14)$$

This leads to an electric field

$$E = \frac{ne u}{\epsilon_0}. \quad (2.15)$$

The displaced electrons thus experience a restoring force which leads to the following equation of motion:

$$nm\ddot{u} = -neE = -\frac{n^2 e^2 u}{\epsilon_0} \quad (2.16)$$

$$\ddot{u} + \omega_p^2 u = 0 \quad (2.17)$$

The plasma frequency thus is the natural frequency of a free oscillation of the electron gas. The quanta of these oscillations are denoted as plasmons.

### 2.1.3 Jellium model

Plasmons can also be analyzed with the formalism of second quantization. In this section, mainly based on [HK09], the superscript for the operators are suppressed and the spin index is assumed to be included in the quasi-momentum subscript. The electron charge density operator

$$\langle \rho_{\vec{q}} \rangle = -\frac{e}{L^3} \sum_{\vec{k}} \langle a_{\vec{k}-\vec{q}}^\dagger a_{\vec{k}} \rangle \quad (2.18)$$

fulfills the following Heisenberg equation of motion [Sak03] :

$$\frac{d}{dt} a_{\vec{k}-\vec{q}}^\dagger a_{\vec{k}} = \frac{i}{\hbar} [H, a_{\vec{k}-\vec{q}}^\dagger a_{\vec{k}}]. \quad (2.19)$$

Here  $a_{\vec{k}}^\dagger$  and  $a_{\vec{k}}$  are the creation and annihilation operators for fermions. They satisfy the following anti-commutation relations:

$$[a_r, a_s^\dagger]_+ = \delta_{rs} \quad (2.20)$$

$$[a_r, a_s]_+ = [a_r^\dagger, a_s^\dagger]_+ = 0. \quad (2.21)$$

$H$  is the Hamilton operator of the electron gas and can be rewritten in terms of these operators

$$H = \sum_{\vec{k}} E_k a_{\vec{k}}^\dagger a_{\vec{k}} + \frac{1}{2} \sum_{\vec{k}, \vec{k}', \vec{q} \neq 0} V_q a_{\vec{k}-\vec{q}}^\dagger a_{\vec{k}'+\vec{q}}^\dagger a_{\vec{k}'} a_{\vec{k}}. \quad (2.22)$$

By calculating the commutator of the Heisenberg equation of motion we find for the kinetic term:

$$\frac{i}{\hbar} \sum_{\vec{k}'} E_{k'} [a_{\vec{k}'}^\dagger a_{\vec{k}'}, a_{\vec{k}-\vec{q}}^\dagger a_{\vec{k}}] = i(\epsilon_{k-q} - \epsilon_k) a_{\vec{k}-\vec{q}}^\dagger a_{\vec{k}} \quad (2.23)$$

with

$$\epsilon_k = E_k/\hbar \quad \text{and} \quad \epsilon_{k-q} = \epsilon_{|\vec{k}-\vec{q}|} = E_{|\vec{k}-\vec{q}|}/\hbar. \quad (2.24)$$

For the Coulomb term we get:

$$\begin{aligned} \sum \frac{iV_p}{2\hbar} [a_{\vec{k}'-\vec{p}}^\dagger a_{\vec{n}+\vec{p}}^\dagger a_{\vec{n}} a_{\vec{k}'}, a_{\vec{k}-\vec{q}}^\dagger a_{\vec{k}}] &= \sum \frac{iV_p}{2\hbar} [a_{\vec{k}-\vec{q}-\vec{p}}^\dagger a_{\vec{n}+\vec{p}}^\dagger a_{\vec{n}} a_{\vec{k}} \\ &- a_{\vec{k}'-\vec{p}}^\dagger a_{\vec{k}-\vec{q}+\vec{p}}^\dagger a_{\vec{k}'} a_{\vec{k}} \\ &+ a_{\vec{k}-\vec{q}}^\dagger a_{\vec{k}'-\vec{p}}^\dagger a_{\vec{k}-\vec{p}} a_{\vec{k}'} \\ &- a_{\vec{k}-\vec{q}}^\dagger a_{\vec{n}+\vec{p}}^\dagger a_{\vec{n}} a_{\vec{k}+\vec{p}}]. \end{aligned} \quad (2.25)$$

Hence,

$$\begin{aligned} \frac{d}{dt} \langle a_{\vec{k}-\vec{q}}^\dagger a_{\vec{k}} \rangle &= i(\epsilon_{k-q} - \epsilon_k) \langle a_{\vec{k}-\vec{q}}^\dagger a_{\vec{k}} \rangle \\ &+ \frac{i}{\hbar} \sum_{\vec{n}, \vec{p}} (\langle a_{\vec{k}-\vec{q}-\vec{p}}^\dagger a_{\vec{n}+\vec{p}}^\dagger a_{\vec{n}} a_{\vec{k}} \rangle \\ &+ \langle a_{\vec{k}-\vec{q}}^\dagger a_{\vec{n}+\vec{p}}^\dagger a_{\vec{k}-\vec{p}} a_{\vec{n}} \rangle). \end{aligned} \quad (2.26)$$

Here the two-operator dynamics is coupled to four operator terms. We therefore split the four-operator expectation values into products of the relevant two-operator expectation values. By using the random phase approximation and keeping  $\langle a_{\vec{k}-\vec{q}}^\dagger a_{\vec{k}} \rangle$  and  $\langle a_{\vec{k}}^\dagger a_{\vec{k}} \rangle = f_{\vec{k}}$  as dynamic variables we find

$$\frac{d}{dt} \langle a_{\vec{k}-\vec{q}}^\dagger a_{\vec{k}} \rangle \cong i(\epsilon_{k-q} - \epsilon_k) \langle a_{\vec{k}-\vec{q}}^\dagger a_{\vec{k}} \rangle + \frac{iV_q}{\hbar} (f_{\vec{k}} - f_{\vec{k}-\vec{q}}) \sum_{\vec{n}} \langle a_{\vec{n}-\vec{q}}^\dagger a_{\vec{n}} \rangle. \quad (2.27)$$

Here  $f_{\vec{k}}$  is the Fermi-Dirac distribution function for electrons in thermodynamic equilibrium. An argument for this approximation is to say that an expectation value  $\langle a_{\vec{k}}^\dagger a_{\vec{k}'} \rangle$  has a time dependence of  $\langle a_{\vec{k}}^\dagger a_{\vec{k}'} \rangle \propto e^{i(\omega_k - \omega_{k'}t)}$ . Under the sums the terms  $\sum_{\vec{k}, \vec{k}'} e^{i(\omega_{\vec{k}} - \omega_{\vec{k}'})t}$  oscillate rapidly for  $k \neq k'$  and so average to zero. To solve for the eigenfrequencies we make the following ansatz

$$\langle a_{\vec{k}-\vec{q}}^\dagger a_{\vec{k}} \rangle(t) = e^{-i(\omega + i\delta)t} \langle a_{\vec{k}-\vec{q}}^\dagger a_{\vec{k}} \rangle(0) \quad (2.28)$$

and get

$$\hbar(\omega + i\delta + \epsilon_{k-q} - \epsilon_k) \langle a_{\vec{k}-\vec{q}}^\dagger a_{\vec{k}} \rangle = V_q (f_{\vec{k}-\vec{q}} - f_{\vec{k}}) \sum_{\vec{n}} \langle a_{\vec{n}-\vec{q}}^\dagger a_{\vec{n}} \rangle. \quad (2.29)$$

This can be rewritten as

$$\langle \rho_{\vec{q}} \rangle = V_q \langle \rho_{\vec{q}} \rangle \sum_{\vec{k}} \frac{f_{\vec{k}-\vec{q}} - f_{\vec{k}}}{\hbar(\omega + i\delta + \epsilon_{k-q} - \epsilon_k)}, \quad (2.30)$$

and  $\langle \rho_{\vec{q}} \rangle$  can be canceled. Then

$$V_q \sum_{\vec{k}} \frac{f_{\vec{k}-\vec{q}} - f_{\vec{k}}}{\hbar(\omega + i\delta + \epsilon_{k-q} - \epsilon_k)} = 1. \quad (2.31)$$

The real part of this equation determines the eigenfrequencies  $\omega = \omega_q$  of the plasma oscillations,

$$V_q \sum_{\vec{k}} \frac{f_{\vec{k}-\vec{q}} - f_{\vec{k}}}{\hbar(\omega_q + \epsilon_{k-q} - \epsilon_k)} = 1. \quad (2.32)$$

To study the long wavelength limit we expand in terms of  $q$ ,

$$\begin{aligned} E_{k-q} - E_k &= \frac{\hbar^2}{2m}(k^2 - 2\vec{k} \cdot \vec{q} + q^2) - \frac{\hbar^2 k^2}{2m} \\ &\simeq -\frac{\hbar^2 \vec{k} \cdot \vec{q}}{m} \end{aligned} \quad (2.33)$$

$$\begin{aligned} f_{\vec{k}-\vec{q}} - f_{\vec{k}} &= f_{\vec{k}} - \vec{q} \cdot \vec{\nabla}_{\vec{k}} f_{\vec{k}} + \dots - f_{\vec{k}} \\ &\simeq -\vec{q} \cdot \vec{\nabla}_{\vec{k}} f_{\vec{k}}. \end{aligned} \quad (2.34)$$

Inserting this into the real part yields

$$\begin{aligned} 1 &\simeq -V_q \sum_{\vec{k}, i} \frac{q_i \frac{\partial f}{\partial k_i}}{\hbar\omega_0 - \hbar^2 \vec{k} \cdot \vec{q}/m} \\ &\simeq -\frac{V_q}{\hbar\omega_0} \sum_{\vec{k}, i} q_i \frac{\partial f}{\partial k_i} \left(1 + \frac{\hbar \vec{k} \cdot \vec{q}}{m\omega_0}\right) \\ &= -\frac{V_q}{\hbar\omega_0} \sum_{k, i} q_i \frac{\partial f}{\partial k_i} \frac{\hbar k \cdot q}{m\omega_0}. \end{aligned} \quad (2.35)$$

Here  $\omega_{q \rightarrow 0} = \omega_0$ . Partial integration gives

$$\begin{aligned} 1 &= V_q \frac{q^2}{m\omega_0^2} \sum_{\vec{k}} f_{\vec{k}} \\ &= V_q \frac{q^2 N}{m\omega_0^2} \\ &= \frac{4\pi e^2}{\epsilon_0 q^2 L^3} \frac{q^2 N}{m\omega_0^2}. \end{aligned} \quad (2.36)$$

Hence

$$\begin{aligned} \omega_0^2 &= \frac{4\pi e^2 n}{m} \\ &= \omega_{pl}^2. \end{aligned} \quad (2.37)$$

This is identical to the result found with the plasma model.

## 2.2 Particle plasmons

If a metallic particle is so small that all points of the particle respond simultaneously to an incoming field, localized surface plasmons can be excited. These resonant surface plasmons on the particle are also called particle plasmons.

### 2.2.1 Surface plasmon polaritons

Surface plasmons are the quanta of surface-charge-density oscillations. They propagate at the interface between a dielectric and a conductor and are confined in perpendicular direction. To describe surface plasmon polaritons we have to look at the central equation of electromagnetic wave theory, which can be obtained by Maxwell's equations. In SI units [Jac98] the macroscopic Maxwell's equations in a linear and isotropic media have the following form

$$\vec{\nabla} \times \vec{E}(\vec{r}, t) = -\frac{\partial \vec{B}(\vec{r}, t)}{\partial t} \quad (2.38)$$

$$\vec{\nabla} \times \vec{H}(\vec{r}, t) = \frac{\partial \vec{D}(\vec{r}, t)}{\partial t} + \vec{j}(\vec{r}, t) \quad (2.39)$$

$$\vec{\nabla} \cdot \vec{D}(\vec{r}, t) = \rho(\vec{r}, t) \quad (2.40)$$

$$\vec{\nabla} \cdot \vec{B}(\vec{r}, t) = 0. \quad (2.41)$$

Here  $\vec{E}(\vec{r}, t)$  is the electric field,  $\vec{D}(\vec{r}, t) = \epsilon_0 \epsilon \vec{E}(\vec{r}, t)$  the electric displacement,  $\vec{H}(\vec{r}, t)$  the magnetic field,  $\vec{B}(\vec{r}, t) = \mu_0 \mu \vec{H}(\vec{r}, t)$  the magnetic induction,  $\vec{j}(\vec{r}, t)$  the current density,  $\rho(r, t)$  the charge density,  $\epsilon$  is the dielectric constant or relative permittivity,  $\mu$  the relative permeability,  $\epsilon_0$  is the electric permittivity and  $\mu_0$  the magnetic permeability of the vacuum. The wave equation is obtained by combining the curls equations

$$\vec{\nabla} \times \vec{\nabla} \times \vec{E} = -\mu_0 \frac{\partial^2 \vec{E}}{\partial t^2}. \quad (2.42)$$

For the absence of  $\rho(\vec{r}, t)$  and  $\vec{j}(\vec{r}, t)$  and negligible variation of the dielectric profile one finds:

$$\vec{\nabla}^2 \vec{E} - \frac{\epsilon}{c^2} \frac{\partial^2 \vec{E}}{\partial t^2} = 0. \quad (2.43)$$

For a harmonic time dependence

$$\vec{E}(\vec{r}, t) = \vec{E}(\vec{r}) e^{-i\omega t} \quad (2.44)$$

we get the Helmholtz equation

$$\vec{\nabla}^2 \vec{E} + k_0^2 \epsilon \vec{E} = 0 \quad (2.45)$$

where  $k_0 = \frac{\omega}{c}$  is the wave number of the propagating wave in vacuum. For a one-dimensional problem  $\epsilon$  depends only on one spatial coordinate. The propagating waves can be described as

$$\vec{E}(x, y, z) = \vec{E}(z) e^{i\beta x}. \quad (2.46)$$

Here  $\beta = k_x$  is the propagation constant which corresponds to the component of the wave vector in the direction of propagation. Inserting into the Helmholtz equation yields

$$\frac{\partial^2 \vec{E}(z)}{\partial z^2} + (k_0^2 \epsilon - \beta^2) \vec{E} = 0. \quad (2.47)$$

A similar equation exists for the magnetic field. To find explicit expressions for the different field components we again use the curl equations. For a propagation along the  $x$ -direction, and assuming homogeneity in the  $y$ -direction and a harmonic time dependence, we arrive at:

$$\frac{\partial E_y}{\partial z} = -i\omega\mu_0 H_x \quad (2.48)$$

$$\frac{\partial E_x}{\partial z} - i\beta E_z = i\omega\mu_0 H_y \quad (2.49)$$

$$i\beta E_y = i\omega\mu_0 H_z \quad (2.50)$$

$$\frac{\partial H_y}{\partial z} = i\omega\epsilon_0\epsilon_0 E_x \quad (2.51)$$

$$\frac{\partial H_x}{\partial z} - i\beta H_z = -i\omega\epsilon_0\epsilon_0 E_y \quad (2.52)$$

$$i\beta H_y = -i\omega\epsilon_0\epsilon_0 E_z \quad (2.53)$$

The system allows two sets of self-consistent solutions. The first set accounts for transverse magnetic modes, where only the field components  $E_x$ ,  $E_z$  and  $H_y$  are nonzero,

$$E_x = -i\frac{1}{\omega\epsilon_0\epsilon} \frac{\partial H_y}{\partial z} \quad (2.54)$$

$$E_z = -\frac{\beta}{\omega\epsilon_0\epsilon} H_y \quad (2.55)$$

$$\frac{\partial^2 H_y}{\partial z^2} + (k_0^2\epsilon - \beta^2)H_y = 0. \quad (2.56)$$

The second set accounts for transverse electric modes, where only the field components  $H_x$ ,  $H_z$  and  $E_y$  are nonzero,

$$H_x = i\frac{1}{\omega\mu_0} \frac{\partial E_y}{\partial z} \quad (2.57)$$

$$H_z = \frac{\beta}{\omega\mu_0} E_y \quad (2.58)$$

$$\frac{\partial^2 E_y}{\partial z^2} + (k_0^2\epsilon - \beta)E_y = 0. \quad (2.59)$$

The simplest geometry where surface plasmon polaritons can exist is a single flat interface between a dielectric, non-absorbing half space with positive real dielectric constant  $\epsilon_2$ , and an adjacent conducting half space with dielectric constant  $\epsilon_1(\omega)$ . Solutions for transverse magnetic modes for  $z > 0$  become

$$H_y(z) = A_2 e^{i\beta x} e^{-k_2 z} \quad (2.60)$$

$$E_x(z) = iA_2 \frac{1}{\omega\epsilon_0\epsilon_2} k_2 e^{i\beta x} e^{-k_2 z} \quad (2.61)$$

$$E_z(z) = -A_1 \frac{\beta}{\omega\epsilon_0\epsilon_2} e^{i\beta x} e^{-k_2 z}. \quad (2.62)$$

Solutions for  $z < 0$  become

$$H_y(z) = A_1 e^{i\beta x} e^{k_1 z} \quad (2.63)$$

$$E_x(z) = -iA_1 \frac{1}{\omega \epsilon_0 \epsilon_1} k_1 e^{i\beta x} e^{k_1 z} \quad (2.64)$$

$$E_z(z) = -A_1 \frac{\beta}{\omega \epsilon_0 \epsilon_1} e^{i\beta x} e^{k_1 z}. \quad (2.65)$$

$k_i$  is the component of the wave vector perpendicular to the interface.  $1/|k_z|$  is the evanescent decay length. Now the boundary conditions at the interface are used. They can be obtained by transforming the Maxwell equations to integral forms by applying the theorems of Stokes and Gauss

$$\int_{\partial S} \vec{E}(\vec{r}, t) \cdot d\vec{s} = - \int_S \frac{\partial}{\partial t} \vec{B}(\vec{r}, t) \cdot \vec{n}_s da \quad (2.66)$$

$$\int_{\partial S} \vec{H}(\vec{r}, t) \cdot d\vec{s} = \int_S [\vec{j}(\vec{r}, t) + \frac{\partial}{\partial t} \vec{D}(\vec{r}, t)] \cdot \vec{n}_s da \quad (2.67)$$

$$\int_{\partial V} \vec{D}(\vec{r}, t) \cdot \vec{n}_s da = \int_V \rho(\vec{r}, t) dV \quad (2.68)$$

$$\int_{\partial V} \vec{B}(\vec{r}, t) \cdot \vec{n}_s da = 0. \quad (2.69)$$

$da$  denotes a surface element,  $n_s$  the normal unit vector to the surface,  $ds$  a line element,  $\partial V$  the surface of the volume  $V$ , and  $\partial S$  the border of the surface  $S$ . To find the boundary conditions the integral forms of Maxwell's equations are applied to a sufficiently small part of the considered boundary. For a arbitrarily small area  $S$  the electric and magnetic fluxes through  $S$  become zero but a surface current density  $K$  might be present. The boundary conditions for the tangential field components are obtained from the first two Maxwell's equations

$$\vec{n} \times (\vec{E}_i - \vec{E}_j) = \vec{0} \quad (2.70)$$

$$\vec{n} \times (\vec{H}_i - \vec{H}_j) = \vec{K}. \quad (2.71)$$

By using Maxwell's third and fourth equations and considering an infinitesimal rectangular box with volume  $V$  and the surface  $\partial V$ , the boundary con-

ditions for the normal field components are obtained as

$$\vec{n} \cdot (\vec{D}_i - \vec{D}_j) = \sigma \quad (2.72)$$

$$\vec{n} \cdot (\vec{B}_i - \vec{B}_j) = 0. \quad (2.73)$$

Here  $\sigma$  is the surface charge density. So  $H_y$  and  $\epsilon_i E_z$  has to be continuous

$$A_1 = A_2 \quad (2.74)$$

$$\frac{k_2}{k_1} = -\frac{\epsilon_2}{\epsilon_1}. \quad (2.75)$$

Confinement to the surface leads to

$$Re[\epsilon_1] < 0 \quad \epsilon_2 > 0. \quad (2.76)$$

$H_y$  also has to fulfill the wave equation:

$$k_1^2 = \beta^2 - k_0^2 \epsilon_1 \quad (2.77)$$

$$k_2^2 = \beta^2 - k_0^2 \epsilon_2. \quad (2.78)$$

This yields the dispersion relation of surface plasmon polaritons which propagate at the interface,

$$\beta = k_0 \sqrt{\frac{\epsilon_1 \epsilon_2}{\epsilon_1 + \epsilon_2}}. \quad (2.79)$$

The wavevector  $k_x$  is always large then the wavevector of light in free space which means that a surface plasmon polariton on a plane interface cannot be excited by light that propagates in free space. However it is possible to excite surface plasmon polaritons in a three-layer system consisting of a thin metal film sandwiched between two insulators of different dielectric constants. Possible configurations are the Kretschmann and the Otto configuration. We refer to [NH06] . It can also be shown that no surface modes exist for transverse electric polarization. Therefore we consider

$$E_y(z) = A_2 e^{i\beta x} e^{-k_2 z} \quad (2.80)$$

$$H_x(z) = -iA_2 \frac{1}{\omega\mu_0} k_2 e^{i\beta x} e^{-k_2 z} \quad (2.81)$$

$$H_z(z) = A_2 \frac{\beta}{\omega\mu_0} e^{i\beta x} e^{-k_2 z} \quad (2.82)$$

for  $z > 0$ , and

$$E_y(z) = A_1 e^{i\beta x} e^{k_1 z} \quad (2.83)$$

$$H_x(z) = iA_1 \frac{1}{\omega\mu_0} k_1 e^{i\beta x} e^{k_1 z} \quad (2.84)$$

$$H_z(z) = A_1 \frac{\beta}{\omega\mu_0} e^{i\beta x} e^{k_1 z} \quad (2.85)$$

for  $z < 0$ . The boundary conditions lead to:

$$A_1(k_1 + k_2) = 0. \quad (2.86)$$

Confinement requires  $Re[k_1] > 0$  and  $Re[k_2] > 0$ . So  $A_1$  and then also  $A_2 = A_1$  has to be zero, which means that no transverse electric modes exist. It is also possible to establish a quantized form of surface plasmons. We refer to [HT08a], [Trü07] and [EQ75].

## 2.2.2 Particle plasmons

Particle plasmons are non-propagating excitations of the conduction electrons of metallic nanostructures coupled to the electromagnetic field. In the discussion we will use the quasi-static approximation in which the particle is much smaller than the wavelength of light in the surrounding medium. The phase of the harmonically oscillating electromagnetic field is practically constant over the particle volume. The most convenient geometry for analyzing the interaction of a particle with an electromagnetic field  $\vec{E} = E_0 \vec{z}$  is a homogeneous, isotropic sphere located at the origin in a uniform, static electric field where the dielectric response of the sphere is described by a dielectric function. In the electrostatic approach, we look for a solution of the Laplace

equation for the potential

$$\frac{1}{r} \frac{\partial^2}{\partial r^2}(r\phi) + \frac{1}{r^2 \sin \theta} \frac{\partial}{\partial \theta} \left( \sin \theta \frac{\partial \phi}{\partial \theta} \right) + \frac{1}{r^2 \sin^2 \theta} \frac{\partial^2 \phi}{\partial \phi^2} = 0. \quad (2.87)$$

It can be solved, if a product form for the potential

$$\phi = \frac{U(r)}{r} P(\theta) Q(\phi) \quad (2.88)$$

is assumed. By using such a product ansatz

$$PQ \frac{d^2 U}{dr^2} + \frac{UQ}{r^2 \sin \theta} \frac{d}{d\theta} \left( \sin \theta \frac{dP}{d\theta} \right) + \frac{UP}{r^2 \sin^2 \theta} \frac{d^2 Q}{d\phi^2} = 0. \quad (2.89)$$

By multiplying with

$$r^2 \sin^2 \theta / UPQ \quad (2.90)$$

we find

$$r^2 \sin^2 \theta \left[ \frac{1}{U} \frac{d^2 U}{dr^2} + \frac{1}{r^2 \sin \theta P} \frac{d}{d\theta} \left( \sin \theta \frac{dP}{d\theta} \right) \right] + \frac{1}{Q} \frac{d^2 Q}{d\phi^2} = 0. \quad (2.91)$$

The last term must be constant:

$$\frac{1}{Q} \frac{d^2 Q}{d\phi^2} = -m^2. \quad (2.92)$$

We find the following solutions for this last term:

$$Q = e^{\pm im\phi}. \quad (2.93)$$

Again by separating the first term we find separate equations for  $P(\theta)$  and  $U(r)$ :

$$\frac{1}{\sin \theta} \frac{d}{d\theta} \left( \sin \theta \frac{dP}{d\theta} \right) + \left[ l(l+1) - \frac{m^2}{\sin^2 \theta} \right] P = 0 \quad (2.94)$$

$$\frac{d^2 U}{dr^2} - \frac{l(l+1)}{r^2} U = 0. \quad (2.95)$$

Here  $l(l+1)$  is a real constant. From the form of the radial equation we find

$$U = Ar^{l+1} + Br^{-l}. \quad (2.96)$$

For a problem with azimuthal symmetry

$$m = 0. \quad (2.97)$$

The general solution then is:

$$\phi(r, \theta) = \sum_{l=0}^{\infty} [A_l r^l + B_l r^{-(l+1)}] P_l(\cos \theta). \quad (2.98)$$

Here  $P_l(\cos \theta)$  are the Legendre-polynomials. For more details see for example [Jac98] or [Has02]. For the solution of the potential inside and outside the sphere we find:

$$\phi_{in}(r, \theta) = \sum_{l=0}^{\infty} [A_l r^l] P_l(\cos \theta) \quad (2.99)$$

$$\phi_{out}(r, \theta) = \sum_{l=0}^{\infty} [B_l r^l + C_l r^{-(l+1)}] P_l(\cos \theta) \quad (2.100)$$

The coefficients can be determined by the boundary conditions

$$-\frac{1}{a} \frac{\partial \phi_{in}}{\partial \theta} \Big|_{r=a} = -\frac{1}{a} \frac{\partial \phi_{out}}{\partial \theta} \Big|_{r=a} \quad (2.101)$$

$$-\epsilon_0 \epsilon \frac{\partial \phi_{in}}{\partial r} \Big|_{r=a} = -\epsilon_0 \epsilon_m \frac{\partial \phi_{out}}{\partial r} \Big|_{r=a} \quad (2.102)$$

$$\phi_{out} = -E_0 z \quad r \rightarrow \infty. \quad (2.103)$$

We find  $B_1 = -E_0$ ,  $B_l = 0$  for  $l \neq 1$  and  $A_l = C_l = 0$  for  $l \neq 1$  and therefore we obtain for the potentials

$$\phi_{in} = \frac{-3\epsilon_m}{\epsilon + 2\epsilon_m} E_0 r \cos \theta \quad (2.104)$$

$$\phi_{out} = -E_0 r \cos \theta + \frac{\epsilon - \epsilon_m}{\epsilon + 2\epsilon_m} E_0 a^3 \frac{\cos \theta}{r^2}. \quad (2.105)$$

The potential outside the sphere is a superposition of a dipole located at the particle center and the applied field. It can therefore be written with the dipole moment  $\vec{p}$ :

$$\phi_{out} = -E_0 r \cos \theta + \frac{\vec{p} \cdot \vec{r}}{4\pi\epsilon_0\epsilon_m r^3} \quad (2.106)$$

$$\vec{p} = 4\pi\epsilon_0\epsilon_m a^3 \frac{\epsilon - \epsilon_m}{\epsilon + 2\epsilon_m} \vec{E}_0. \quad (2.107)$$

Here  $a$  is the radius of the sphere. The polarizability

$$\alpha = 4\pi a^3 \frac{\epsilon - \epsilon_m}{\epsilon + 2\epsilon_m} \quad (2.108)$$

defined via

$$\vec{p} = \epsilon_m \epsilon_0 \alpha \vec{E}_0 \quad (2.109)$$

experiences a resonant enhancement under the condition that  $|\epsilon + 2\epsilon_m|$  is a minimum, which, for the case of small or slowly-varying  $Im[\epsilon]$  around the resonance, simplifies to

$$Re[\epsilon(\omega)] = -2\epsilon_m. \quad (2.110)$$

This is called the Fröhlich condition. The associated mode is the dipole surface plasmon. The surface plasmon resonance depends on the particle shape, the dielectric function of the metal, and on the dielectric function of the environment. So metallic nanoparticles can be used for optical sensing.

## Optical sensing

The electric fields are evaluated from the potentials:

$$\vec{E} = -\vec{\nabla}\phi \quad (2.111)$$

$$\vec{E}_{in} = \frac{3\epsilon_m}{\epsilon + 2\epsilon_m} \vec{E}_0 \quad (2.112)$$

$$\vec{E}_{out} = \vec{E}_0 + \frac{3\vec{n}(\vec{n} \cdot \vec{p}) - \vec{p}}{4\pi\epsilon_m\epsilon_0} \frac{1}{r^3}. \quad (2.113)$$

The scattered field is identical to the electric field of a dipole:

$$\vec{E} = \frac{1}{4\pi\epsilon_0\epsilon_m} (k^2(\vec{n} \times \vec{p}) \times \vec{n} \frac{e^{ikr}}{r} + [3\vec{n}(\vec{n} \cdot \vec{p}) - \vec{p}] (\frac{1}{r^3} - \frac{ik}{r^2}) e^{ikr}) \quad (2.114)$$

$$\vec{E} = \frac{3\vec{n}(\vec{n} \cdot \vec{p}) - \vec{p}}{4\pi\epsilon_0\epsilon_m} \frac{1}{r^3} \quad kr \ll 1. \quad (2.115)$$

Here  $k = 2\pi/\lambda$  and  $\vec{n}$  is the unit vector to the point of interest. The illumination with a plane wave

$$\vec{E}(\vec{r}, t) = E_0 e^{-i\omega t} \quad (2.116)$$

induces an radiating oscillating dipole

$$\vec{p} = \epsilon_0\epsilon_m\alpha E_0 e^{-i\omega t} \quad (2.117)$$

which leads to a scattering of the plane wave. The corresponding scattering and absorption cross sections are given by

$$C_{sca} = \frac{8\pi}{3} k^4 a^6 \left| \frac{\epsilon - \epsilon_m}{\epsilon + 2\epsilon_m} \right|^2 \quad (2.118)$$

$$C_{abs} = 4\pi k a^3 \text{Im} \left[ \frac{\epsilon - \epsilon_m}{\epsilon + 2\epsilon_m} \right]. \quad (2.119)$$

The sum of scattering and absorption is the extinction.

$$C_{ext} = C_{sca} + C_{abs}. \quad (2.120)$$

$C_{sca}$  and  $C_{abs}$  scale differently. The extinction and therefore the color depends on the size of the particles. A nice illustration is given by the Lycurgus cup. Because of the plasmonic excitation in the metallic particles in the glass of the cup it absorbs and scatters blue and green light. When viewed in reflected light, the plasmonic scattering gives the cup a green color, but if a white light source is placed within the cup, the glass appears red because it transmits only the longer wavelengths and absorbs the shorter ones 2.1 . We refer to [NH06], [Mai07] and [Sqa02].

## 2.3 Boundary element method

Boundary integral equations and the boundary element method are methods for numerical analysis in science. There exist different implementations of boundary integral methods. The direct methods relate the volume integration directly by using Green's second theorem to a surface integration. The indirect method is based on an ad-hoc solution with some auxiliary quantities which are chosen such that the appropriate boundary conditions are fulfilled. In the boundary element method the surface is approximated by small surface elements of triangular or rectangular shape. In this section Gauss units are used. We refer to [HK05] and [Wro02].

### Direct method

The problem considered in this and the following sections is the solution of the free Helmholtz equation

$$[\vec{\nabla}^2 + k^2\epsilon(\vec{r})]\phi(\vec{r}) = 0. \quad (2.121)$$

Here  $k$  is the photon wave vector in vacuum,  $\phi(\vec{r})$  is the scalar potential and  $\epsilon(\vec{r})$  is the dielectric function. In the direct method the Helmholtz equation and the equation for the Green functions  $G_j(\vec{r}, \vec{r}')$

$$(\vec{\nabla}^2 + k_j^2\epsilon_j)G_j(\vec{r}, \vec{r}') = -4\pi\delta(\vec{r} - \vec{r}'), \quad \vec{r}, \vec{r}' \in \Omega_j, \quad (2.122)$$

are combined in such a way that  $\phi(\vec{r})$  can be computed from the knowledge of  $\phi$  and its surface derivative at the boundary. By using Green's second theorem we get:

$$4\pi\phi(\vec{r}) = \int_{\partial\Omega_j} d\vec{s}' \vec{n}_j(\vec{s}') [G_j(\vec{r}, \vec{s}') \vec{\nabla}_{s'} \phi(\vec{s}') - \phi(\vec{s}') \vec{\nabla}_{s'} G_j(\vec{r}, \vec{s}')]. \quad (2.123)$$

Here  $\vec{n}_j(\vec{s})$  is the outer surface normal.  $\phi$  and its surface derivative at the boundary are determined in two steps. First, one performs the limit  $\vec{r} \rightarrow \vec{s}$

$$2\pi\phi(\vec{s}) = \int_{\partial\Omega_j} d\vec{s}' \vec{n}_j(\vec{s}') [G_j(\vec{s}, \vec{s}') \vec{\nabla}_{s'} \phi(\vec{s}') - \phi(\vec{s}') \vec{\nabla}_{s'} G_j(\vec{r}, \vec{s}')]. \quad (2.124)$$

In the second step, this integral equation is combined with the boundary conditions imposed by the Maxwell's equations to obtain  $\phi(\vec{s})$  and  $\vec{n}_j(\vec{s}) \cdot \vec{\nabla}_s \phi(\vec{s})$ .

$$(2.125)$$

### Indirect method

Here the solution of the free Helmholtz equation is written in the ad hoc form

$$\phi(\vec{r}) = \phi_j^e(\vec{r}) + \int_{\partial\Omega_j} d\vec{s} G_j(\vec{r}, \vec{s}') \sigma_j(\vec{s}'), \quad \vec{r} \in \Omega_j, \quad (2.126)$$

with  $\phi_j^e(\vec{r})$  a solution of the free Helmholtz equation and  $\sigma_j(\vec{s})$  a surface charge.

### Retarded case

The following derivation is based on [GH02] and [GH98]. It starts from the Maxwell's equations in frequency space  $\omega$ :

$$\vec{\nabla} \cdot \vec{D} = 4\pi\rho \quad (2.127)$$

$$\vec{\nabla} \times \vec{H} + ik\vec{D} = \frac{4\pi}{c} \vec{j} \quad (2.128)$$

$$\vec{\nabla} \cdot \vec{B} = 0 \quad (2.129)$$

$$\vec{\nabla} \times \vec{E} - ik\vec{B} = 0. \quad (2.130)$$

Here  $k = \omega/c$  is the wave vector,  $\vec{D} = \epsilon\vec{E}$  is the electric displacement, and  $\vec{B} = \mu\vec{H}$  is the magnetic induction. The electric and magnetic fields  $\vec{E}$  and

$\vec{H}$  can be expressed in terms of scalar and vector potentials  $\phi$  and  $\vec{A}$ .

$$\vec{E} = ik\vec{A} - \vec{\nabla}\phi \quad (2.131)$$

$$\vec{H} = \frac{1}{\mu}\vec{\nabla} \times \vec{A} \quad (2.132)$$

By using the Lorentz gauge

$$\vec{\nabla} \cdot \vec{A} = ik\epsilon\mu\phi \quad (2.133)$$

the first two Maxwell equations can be rewritten

$$(\vec{\nabla}^2 + k^2\epsilon\mu)\phi = -4\pi\left(\frac{\rho}{\epsilon} + \frac{1}{4\pi}\vec{D} \cdot \vec{\nabla}\frac{1}{\epsilon}\right) \quad (2.134)$$

$$(\vec{\nabla}^2 + k^2\epsilon\mu)\vec{A} = -\frac{4\pi}{c}(\mu\vec{j} - \frac{1}{4\pi}[i\omega\phi\vec{\nabla}(\epsilon\mu) + c\vec{H} \times \vec{\nabla}\mu]). \quad (2.135)$$

where  $\sigma_s = +\frac{1}{4\pi}\vec{D}\vec{\nabla}\frac{1}{\epsilon}$  and  $m = -\frac{1}{4\pi}[i\omega\phi\vec{\nabla}(\epsilon\mu) + c\vec{H} \times \vec{\nabla}\mu]$  can be understood as additional charges and currents on the interfaces of the dielectric bodies.

The general solutions are

$$\phi(\vec{r}) = \frac{1}{\epsilon_j(\omega)} \int d\vec{r}' G_j(|\vec{r} - \vec{r}'|) \rho(\vec{r}') + \int_{S_j} ds G_j(|\vec{r} - \vec{s}'|) \sigma_j(\vec{s}') \quad (2.136)$$

$$\vec{A}(\vec{r}) = \frac{\mu_j(\omega)}{c} \int d\vec{r}' G_j(|\vec{r} - \vec{r}'|) \vec{j}(\vec{r}') + \int_{S_j} d\vec{s}' G_j(|\vec{r} - \vec{s}'|) \vec{h}_j(\vec{s}') \quad (2.137)$$

with  $S_j$  the boundary of the medium, and  $G_j(r) = \frac{e^{ik_j r}}{r}$  the Green function of the wave equation  $[\vec{\nabla}^2 + k_j^2]G_j(r) = -4\pi\delta(\vec{r})$ . The boundary conditions and the gauge conditions lead to:

$$G_1\sigma_1 - G_2\sigma_2 = \phi_2^e - \phi_1^e \quad (2.138)$$

$$G_1\vec{h}_1 - G_2\vec{h}_2 = \vec{A}_2^e - \vec{A}_1^e. \quad (2.139)$$

Here

$$\phi_j^e(\vec{s}') = \frac{1}{\epsilon_j(\omega)} \int d\vec{r}' G_j(|\vec{s}' - \vec{r}'|) \rho(\vec{r}') \quad (2.140)$$

and

$$\vec{A}_j^e(\vec{s}) = \frac{\mu_j(\omega)}{c} \int d\vec{r}' G_j(|\vec{s} - \vec{r}'|) \vec{j}(\vec{r}') \quad (2.141)$$

are equivalent boundary sources that scale linearly with the external perturbation. Because of the boundary conditions the tangential derivatives of all components of the vector potential and the normal derivative of the tangential vector potential must be continuous in the nonmagnetic case.

$$(\vec{n}_s \vec{\nabla}) \vec{A} - i\vec{n}_s k \epsilon \mu \phi \quad (2.142)$$

has to be continuous. By inserting the general solutions in this last relation we find:

$$H_1 \vec{h}_1 - H_2 \vec{h}_2 - ik\vec{n}_s (G_1 \epsilon_1 \mu_1 \sigma_1 - G_2 \epsilon_2 \mu_2 \sigma_2) = \vec{\alpha} \quad (2.143)$$

$$\vec{\alpha} = (\vec{n}_s \cdot \vec{\nabla})(\vec{A}_2^e - \vec{A}_1^e) + ik\vec{n}_s (\epsilon_1 \mu_1 \phi_1^e - \epsilon_2 \mu_2 \phi_2^e) \quad (2.144)$$

with

$$\begin{aligned} H_j(\vec{s}, \vec{s}') &= \lim_{\eta \rightarrow 0^+} \vec{n}_s \cdot \vec{\nabla}_s G_j(|\vec{s} \mp \eta \vec{n}_s - \vec{s}'|) \\ &= \vec{n}_s \cdot \vec{\nabla}_s G_j(|\vec{s} - \vec{s}'|) \pm 2\pi \delta(\vec{s} - \vec{s}') \end{aligned} \quad (2.145)$$

$$\vec{n}_s \cdot \vec{\nabla}_s G_j(|\vec{s} - \vec{s}'|) = \frac{\vec{n}_s(\vec{s} - \vec{s}')}{|\vec{s} - \vec{s}'|^3} (ik_j |\vec{s} - \vec{s}'| - 1) e^{ik_j |\vec{s} - \vec{s}'|}. \quad (2.146)$$

For magnetic materials the tangential part takes the form

$$\begin{aligned} (\vec{n}_s \partial_i G_1 - \vec{t}_s^i H_1) \frac{1}{\mu_1} \cdot \vec{h}_1 - (\vec{n}_s \partial_i G_2 - \vec{t}_s^i H_2) \frac{1}{\mu_2} \cdot \vec{h}_2 &= [\vec{n}_s \partial_i - \vec{t}_s^i \cdot (\vec{n}_s \cdot \vec{\nabla}_s)] \\ &\times \left( \frac{\vec{A}_2^e}{\mu_2} - \frac{\vec{A}_1^e}{\mu_1} \right). \end{aligned} \quad (2.147)$$

Here  $\vec{t}_s^1$  and  $\vec{t}_s^2$  are two independent tangential vectors and the derivative  $\partial_i$  is taken along the direction  $\vec{t}_s^i$ . The continuity of the normal electric displacement

$$\epsilon \vec{n}_s \cdot (ik\vec{A} - \vec{\nabla} \phi) \quad (2.148)$$

leads to

$$H_1\epsilon_1\sigma_1 - H_2\epsilon_2\sigma_2 - ik\vec{n}_s(G_1\epsilon_1\vec{h}_1 - G_2\epsilon_2\vec{h}_2) = D^e \quad (2.149)$$

$$D^e = \vec{n}_s \cdot [\epsilon_1(ik\vec{A}_1^e - \vec{\nabla}_s\phi_1^e) - \epsilon_2(ik\vec{A}_2^e - \vec{\nabla}_s\phi_2^e)]. \quad (2.150)$$

The boundary charges and currents needed for the general solutions can be calculated self-consistently.

### Non retarded case

In the non retarded limit,  $k \rightarrow 0$ , the Green function reduces to the non-retarded Coulomb interaction  $1/r$ .  $\phi_j^e$  becomes independent of  $j$ .  $\vec{A}_j^e$  and  $\vec{\alpha}$  vanish. Hence

$$D^e = (\epsilon_2 - \epsilon_1)f \quad (2.151)$$

with

$$f(\vec{s}) = \int d\vec{r}' F(\vec{s}, \vec{r}') \frac{\rho(\vec{r}')}{\epsilon(\vec{r}', \omega)} \quad (2.152)$$

$$F(\vec{s}, \vec{s}') = -\frac{\vec{n}_s \cdot (\vec{s} - \vec{s}')}{|\vec{s} - \vec{s}'|^3} \quad (2.153)$$

the external electric field normal to the interface. The continuity of the tangential electric field and the normal magnetic induction at the interface and the gauge condition are satisfied by  $\vec{h}_j = 0$  and  $\sigma_1 = \sigma_2 = \sigma$ . For the continuity of the normal electric displacement we get

$$\Lambda\sigma(\vec{s}) = f(\vec{s}) + \int_S d\vec{s}' F(\vec{s}, \vec{s}')\sigma(\vec{s}') \quad (2.154)$$

with

$$\Lambda = 2\pi \frac{\epsilon_2 + \epsilon_1}{\epsilon_2 - \epsilon_1}. \quad (2.155)$$

From this equation the induced surface charge can be calculated self-consistently.

The induced potential is given in terms of the induced interface charge

$$\phi^{ind}(\vec{r}) = \int d\vec{s}' \frac{\sigma(\vec{s}')}{|\vec{r} - \vec{s}'|}. \quad (2.156)$$

## 2.4 Plasmon dynamics

The boundary element method can be used to study the plasmon dynamics of a metallic nanoparticle illuminated by a plane wave. In the non retarded case the solution for  $\phi(\vec{r})$  is given by

$$\phi(\vec{r}) = \int_{\partial\Omega} G(\vec{r}, \vec{s}') \sigma(\vec{s}') ds' + \phi_{ext}. \quad (2.157)$$

For using the boundary condition of the continuity of the tangential electric field the surface derivative on both sides of the boundary has to be taken. One finds

$$\lim_{\vec{r} \rightarrow \vec{s}} \phi'(r) = \int_{\partial\Omega} F(\vec{s}, \vec{s}') \sigma(\vec{s}') \pm 2\pi\sigma(\vec{s}) + \phi'_{ext}(\vec{s}) \quad (2.158)$$

with

$$\phi' = (\hat{n} \cdot \vec{\nabla}) \phi \quad (2.159)$$

and

$$F(\vec{s}, \vec{s}') = (\hat{n} \cdot \vec{\nabla}) G(\vec{s}, \vec{s}'). \quad (2.160)$$

By approximating the surface of the nanoparticle by surface elements, the integral equation reduces to two matrix equations:

$$\phi'_m = (F + 2\pi 1)\sigma + \phi'_{ext} \quad (2.161)$$

$$\phi'_b = (F - 2\pi 1)\sigma + \phi'_{ext}. \quad (2.162)$$

Then by using the boundary condition

$$\epsilon_m \phi'_m - \epsilon_b \phi'_b = 0 \quad (2.163)$$

the equation for the surface charge can be calculated

$$\sigma = -[2\pi(\epsilon_m + \epsilon_b)\hat{1} + (\epsilon_m - \epsilon_b)\hat{F}]^{-1}(\epsilon_m - \epsilon_b)\phi'_{ext} \quad (2.164)$$

$$\Lambda\sigma = F\sigma + \phi'_{ext} \quad (2.165)$$

with

$$\Lambda = 2\pi \frac{\epsilon_b + \epsilon_m}{\epsilon_b - \epsilon_m}. \quad (2.166)$$

For a given  $\sigma$  the induced dipole moment  $d = \sum_i s_i \sigma_i$  can be computed. Further one finds the following eigenvalue equations

$$F\sigma_k = \lambda_k \sigma_k \quad (2.167)$$

$$\tilde{\sigma}_k F = \lambda_k \tilde{\sigma}_k, \quad (2.168)$$

where  $\lambda_k$  are real eigenvalues and  $\sigma_k$  and  $\tilde{\sigma}_k$  are the left and right eigenvectors. For a symmetric matrix the left and the right eigenvectors are just its transpose [Pre07]. In [MZM02] [MFZ05] [FM03] it is shown that they are biorthogonal. They can be used for an expansion of the surface charge

$$\sigma(s, t) = \sum_k a_k(t) \sigma_k(s) \quad (2.169)$$

$$a_k(t) = \int_{\partial\Omega} \tilde{\sigma}_k(s) \sigma(s, t) ds. \quad (2.170)$$

We find:

$$(\Lambda - F) \sum_{k'} a_{k'} \sigma_{k'} = \phi'_{ext} \quad (2.171)$$

$$\sum_{k'} a_{k'} (\Lambda - \lambda_{k'}) \sigma_{k'} = \phi'_{ext}. \quad (2.172)$$

Then by multiplying with

$$\int_{\partial\Omega} ds \tilde{\sigma}_k(s) \quad (2.173)$$

we find an expression for the expansion coefficient which reveals the dynamics of the localized surface plasmon

$$a_k(\omega) = \frac{1}{\Lambda(\omega) - \lambda_k} \int_{\partial\Omega} \tilde{\sigma}_k(s) \phi'_{ext}(s, \omega) ds. \quad (2.174)$$

## 2.5 Electric dipole interactions

The properties of local surface plasmon resonances depend on interparticle coupling. We consider an exciting system consisting of a metallic nanoparticle coupled to a molecule with a certain dipole moment in a given direction,

$$d = f(\omega)E. \quad (2.175)$$

Then

$$E = E_{inc} + E_{inc}^{MNP} + E_{dip}^{MNP} \quad (2.176)$$

is the sum of the electric field of the external source and the electric field of the metallic nanoparticle and

$$f(\omega) = \left(\frac{q}{m}\right) \left(\frac{1}{\omega_0^2 - i\gamma_0\omega - \omega^2}\right) \quad (2.177)$$

is the dipole response function which is found from the equation of motion

$$\ddot{\vec{x}}(t) + \gamma_0\dot{\vec{x}}(t) + \omega_0^2\vec{x}(t) = \frac{q}{m}(\vec{E}(t)). \quad (2.178)$$

Hence we find

$$d = f(\omega)(E_{inc} + E_{inc}^{MNP} + dE_{dip}^{MNP}) \quad (2.179)$$

$$d(1 - E_{dip}^{MNP}) = f(\omega)(E_{inc} + E_{inc}^{MNP}) \quad (2.180)$$

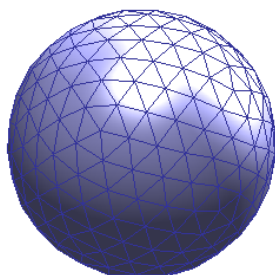
$$d = \frac{f(\omega)(E_{inc} + E_{inc}^{MNP})}{(1 - E_{dip}^{MNP})}. \quad (2.181)$$

Complex structures often yield multi-featured resonance spectra. This can be seen as the result of a hybridization of elementary plasmons of simpler substructures. Another effect which appears at hybrid structures is the non-linear Fano effect. It is caused from the interference between the external field and the induced internal field. Then the absorption intensity can have a strongly asymmetric shape. We refer to [KG08] and [ZG06].

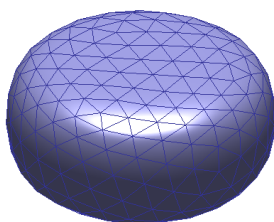
## Results

Figure 2.2 shows the approximation of different types of metallic nanoparticles with triangles within the boundary element method. In the most simple form, the surface charges are at the center of each triangle and the matrices  $G_{ij}$  and  $F_{ij}$  connect the different surface elements. Figure 2.3 shows dipole surface plasmon eigenmodes for a spherical gold nanoparticle with the diameter  $a = 10$  nm. For gold the dielectric function of [JC72] and for the background dielectric function water with  $\epsilon_{out} = 1.33^2$  was used. Figure 2.4 shows the scattered normalized intensity of spherical metallic nanoparticles with diameter  $a = 10$  nm computed within the nonretarded approach. For gold the drude dielectric function was used. For the background the dielectric functions of glass  $\epsilon_{out} = 1.5^2$ , water  $\epsilon_{out} = 1.33^2$  and vacuum  $\epsilon_{out} = 1$  were used. The conversion factor between energy eV and  $\lambda$  nm is given by  $E = h\frac{c}{\lambda} \rightarrow E \text{ eV} = 1239.84 \frac{1}{\lambda \text{ nm}}$ . A redshift of the resonance is observed if the dielectric constant of the environment is increased. In figure 2.5 the normalized scattered intensity for a coupled system consisting of a spherical gold nanoparticle and a dipole in  $x$ -direction with length  $\eta = 1 \cdot 10^{-9}$  nm which is excited with  $x$ -polarized light from the  $x$ -direction is shown. The different plots distinguish between the different positions of  $z = 1 \cdot d$ ,  $z = 1.2 \cdot d$  and  $z = 1.4 \cdot d$ , where  $d$  is the diameter of the nanoparticle, of the dipole. The resonance energy of the dipole was chosen at 2.4 eV. The diameter of the nanoparticle was chosen at 10 nm. For gold the drude dielectric function and for the background the dielectric function of glass  $\epsilon_{out} = 1.5^2$  was used. The energy shifts and broadens for different interparticle distances. The shift depends on polarization of the exciting light as well. We refer to [KB07] and [HK05].

Sphere



Disk



Cube

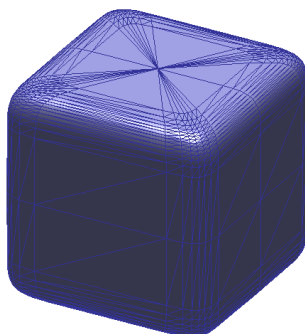


Figure 2.2: Different shapes of metal nanoparticles approximated by a set of triangles.

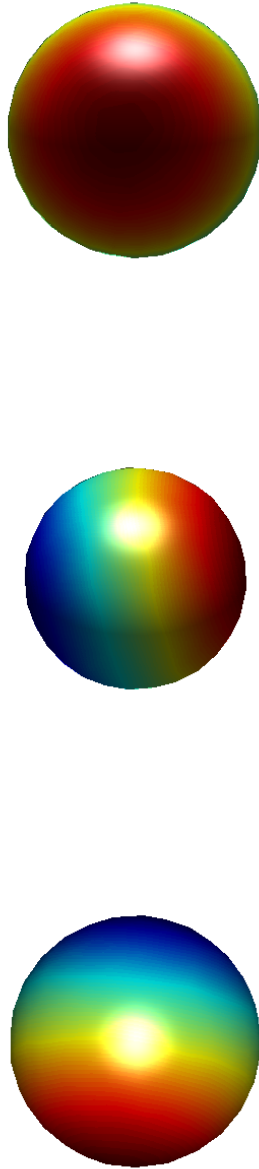


Figure 2.3: Here the dipole surface plasmon eigenmodes for a spherical gold nanoparticle with the diameter  $a = 10$  nm are shown. For gold the dielectric function of [JC72] was used.

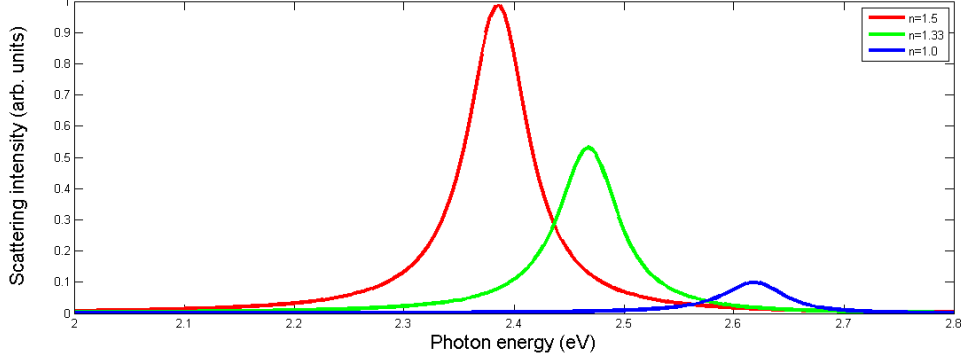


Figure 2.4: The scattered intensity of a spherical gold nanoparticle in different environments is shown. For the background the dielectric functions of glass  $\epsilon_{out} = 1.5^2$ , water  $\epsilon_{out} = 1.33^2$  and vacuum  $\epsilon_{out} = 1$  were used. A redshift of the resonance is observed if the dielectric constant of the environment is increased.

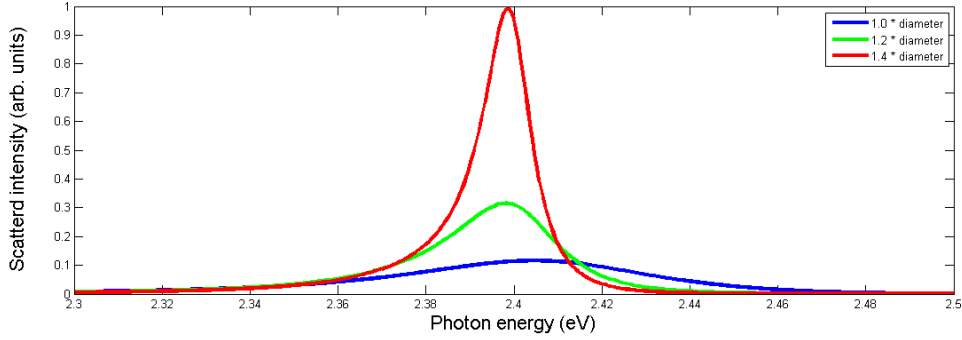


Figure 2.5: Scattered intensity for a coupled system consisting of a spherical metallic nanoparticle and a dipole in  $x$ -direction with length  $\eta = 1 \cdot 10^{-9}$  nm which is excited with  $x$ -polarized light from the  $x$ -direction is shown. The different plots distinguish between the different positions of  $z = 1 \cdot d$ ,  $z = 1.2 \cdot d$  and  $z = 1.4 \cdot d$ , where  $d$  is the diameter of the nanoparticle, of the dipole. The resonance energy of the dipole was chosen at 2.4 eV. The diameter of the nanoparticle was chosen at 10 nm. For gold the drude dielectric function and for the background the dielectric function of glass  $\epsilon_{out} = 1.5^2$  was used. The energy shifts and broadens for different interparticle distances. The shift depends on polarization of the exciting light as well.



# Chapter 3

## Carbon nanotubes

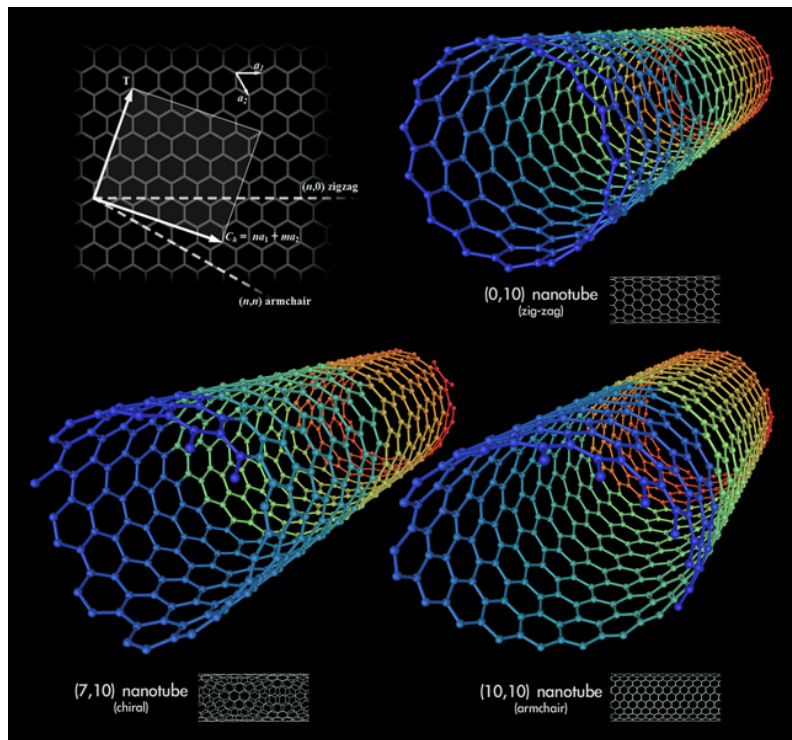


Figure 3.1: In this figure the three different types of carbon nanotubes are shown. The integers  $n$  and  $m$  of the chiral vector  $\vec{C} = (n, m)$  define the tubes.  $(n, 0)$  are called zigzag,  $(n, n)$  are called armchair and  $(n, m)$  are chiral tubes.  
source: [www.nanoscienceworks.org](http://www.nanoscienceworks.org)

## 3.1 Carbon nanotubes

Carbon nanotubes are cylinders of graphite sheets [Iij91]. Two possible methods to synthesize them are the laser vaporization and the carbon arc synthesis. Carbon nanotubes have a diameter of some nanometers and a length of some millimeters. Because of their special structure they have certain properties that make them potentially useful in many applications in nanotechnology. For example, they have the highest strength to weight ratio of any known material and can penetrate membranes such as cell walls which makes them useful in material science and medical applications. We refer to [Rei03], [Sai99], [CBR07] and [Zar08].

### 3.1.1 Electronic structure of graphene

The characteristic band structure of a solid can be studied from two different limiting cases. In combining free atoms to a crystal the discrete atom levels split up in groups and the influence of a lattice potential breaks the continuous spectrum of a free electron gas. The tight binding method is an approximation method which starts by expressing the Bloch functions as a linear combination of atomic orbitals. This and the following sections are mainly based on [Zar08].

#### Tight binding

As already mentioned in the tight binding method the Bloch functions are written as a linear combination of atomic orbitals

$$\phi_{st}(\vec{k}, \vec{r}) = \frac{1}{\sqrt{N}} \sum_l^N e^{i\vec{k} \cdot \vec{R}_{ls}} \psi_t(\vec{r} - \vec{R}_{ls}), \quad t = 1, \dots, n. \quad (3.1)$$

Here  $\psi_t(\vec{r} - \vec{R}_{ls})$  is the atomic wave function in state  $t$ ,  $\vec{R}_{ls}$  is the position vector of the  $s$ th atom in the  $l$ th primitive unit cell,  $n$  is the number of atomic wave functions in the unit cell, and  $N$  is the number of unit cells of the crystal. The eigenfunctions of the solid are expressed as linear combinations of the

Bloch functions

$$\Psi_j(\vec{k}, \vec{r}) = \sum_s C_{js}(\vec{k}) \phi_s(\vec{k}, \vec{r}) \quad (3.2)$$

with the expansion coefficients  $C_{js}(\vec{k})$ . To find the eigenfunctions and eigenvalues of a Hamiltonian the coefficients are chosen such that the expectation value of the Hamiltonian with these functions takes a minimum. This is done by solving the so called secular equation

$$\det[\hat{H} - E_{\vec{k}} \hat{S}] = 0. \quad (3.3)$$

Here the elements of the Hamilton matrices  $\hat{H}$  are given by

$$\begin{aligned} H_{jj'}(\vec{k}) &= \langle \phi_j(\vec{k}, \vec{r}) | \hat{H} | \phi_{j'}(\vec{k}, \vec{r}) \rangle \\ &= \frac{1}{N} \sum_{st} e^{i\vec{k} \cdot (\vec{R}_{sj'} - \vec{R}_{tj})} \langle \psi(\vec{r} - \vec{R}_{tj}) | \hat{H} | \psi(\vec{r} - \vec{R}_{sj'}) \rangle. \end{aligned} \quad (3.4)$$

For the overlap matrices one finds:

$$\begin{aligned} S_{jj'}(\vec{k}) &= \langle \phi_j(\vec{k}, \vec{r}) | \phi_{j'}(\vec{k}, \vec{r}) \rangle \\ &= \frac{1}{N} \sum_{st} e^{i\vec{k} \cdot (\vec{R}_{sj'} - \vec{R}_{tj})} \langle \psi(\vec{r} - \vec{R}_{tj}) | \psi(\vec{r} - \vec{R}_{sj'}) \rangle. \end{aligned} \quad (3.5)$$

## Tight binding of graphene

In this section the tight binding method is used to calculate the dispersion relation of graphene. With the dispersion relation of graphene and zone folding the dispersion relation of a single wall carbon nanotube can be calculated. Graphene is a one-atom-thick planar sheet of  $sp^2$ -bonded carbon atoms that are densely packed in a honeycomb crystal lattice. In graphene each carbon atom has three  $2sp^2$  electrons and one  $2p$  electron. The  $2sp^2$  electrons form the three bonds in the plane of the sheet and the  $p_z$  orbital perpendicular to the sheet forms  $\pi$  covalent bonds, which are responsible for the electronic properties. For a discussion of the physics of atoms and molecules we refer to [HW05]. The unit cell of graphene has two carbon atoms. Its wave function

can be written as a sum of two Bloch functions

$$\Psi_j(\vec{k}, \vec{r}) = \sum_{A,B} C_{js}(\vec{k}) \phi_s(\vec{k}, \vec{r}). \quad (3.6)$$

The general form of the secular equation is found by the Schrödinger equation

$$\hat{H}\Psi_j(\vec{k}, \vec{r}) = E_j(\vec{k})\Psi_j(\vec{k}, \vec{r}). \quad (3.7)$$

Written with the Bloch functions it takes the following form:

$$\begin{aligned} C_{jA}(\vec{k})\hat{H}\phi_A(\vec{k}, \vec{r}) + C_{jB}(\vec{k})\hat{H}\phi_B(\vec{k}, \vec{r}) &= C_{jA}(\vec{k})E_j(\vec{k})\phi_A(\vec{k}, \vec{r}) \\ &+ C_{jB}(\vec{k})E_j(\vec{k})\phi_B(\vec{k}, \vec{r}). \end{aligned} \quad (3.8)$$

Now multiplying with  $\phi_A(\vec{k}, \vec{r})$  and  $\phi_B(\vec{k}, \vec{r})$  the secular equation is found:

$$\begin{vmatrix} H_{AA}(\vec{k}) - E_j(\vec{k})S_{AA}(\vec{k}) & H_{AB}(\vec{k}) - E_j(\vec{k})S_{AB}(\vec{k}) \\ H_{AB}^* - E_j(\vec{k})S_{AB}^*(\vec{k}) & H_{AA}(\vec{k}) - E_j(\vec{k})S_{AA}(\vec{k}) \end{vmatrix} = 0. \quad (3.9)$$

Using the tight binding method the overlap matrix is

$$H_{AB}(\vec{k}) = \frac{1}{N} \sum_{st} e^{i\vec{k}\cdot(\vec{R}_{sB}-\vec{R}_{tA})} \langle \psi(\vec{r}-\vec{R}_{tA}) | \hat{H} | \psi(\vec{r}-\vec{R}_{sB}) \rangle. \quad (3.10)$$

Changing the variable of integration from  $\vec{r}$  to  $\vec{r}' = \vec{r} - \vec{R}_{tA}$  and after that dropping the prime, one obtains

$$\begin{aligned} H_{AB}(\vec{k}) &= \frac{1}{N} \sum_{st} e^{i\vec{k}\cdot(\vec{R}_{sB}-\vec{R}_{tA})} \langle \psi(\vec{r}') | \hat{H} | \psi(\vec{r}' - (\vec{R}_{sB} - \vec{R}_{tA})) \rangle \\ &= \frac{1}{N} \sum_{tl} e^{i\vec{k}\cdot\vec{b}_l^A} \langle \psi(\vec{r}') | \hat{H} | \psi(\vec{r}' - \vec{b}_l^A) \rangle \\ &= \sum_{l=1}^3 e^{-i\vec{k}\cdot\vec{b}_l^A} \langle \psi(\vec{r}') | \hat{H} | \psi(\vec{r}' + \vec{b}_l^A) \rangle \\ &= \gamma_0 f(\vec{k}) \end{aligned} \quad (3.11)$$

$$H_{BA}(\vec{k}) = H_{AB}^*(\vec{k}). \quad (3.12)$$

Here  $\vec{b}_l^A, l = 1, 2, 3$  are the nearest-neighbor carbon atom vectors with the bond length  $|\vec{b}_l^A| = a/\sqrt{3}$ ,

$$\begin{aligned} f(\vec{k}) &= \sum_{l=1}^3 e^{-i\vec{k}\cdot\vec{b}_l^A} \\ &= e^{-ik_x a/\sqrt{3}} + 2e^{ik_x a/2\sqrt{3}} \cos(k_y a/2), \end{aligned} \quad (3.13)$$

and

$$\gamma_0 = \langle \psi(\vec{r}) | \hat{H} | \psi(\vec{r} + \vec{b}_l^A) \rangle \quad (3.14)$$

is the transfer integral. In similar way the other matrix elements become

$$\begin{aligned} H_{AA}(\vec{k}) &= H_{BB}(\vec{k}) \\ &= \frac{1}{N} \sum_{st} e^{i\vec{k}\cdot(\vec{R}_{sA}-\vec{R}_{tA})} \langle \psi(\vec{r}) | \hat{H} | \psi(\vec{r} - (\vec{R}_{sA} - \vec{R}_{tA})) \rangle \\ &\approx \langle \psi(\vec{r}) | \hat{H} | \psi(\vec{r}) \rangle \\ &= \epsilon_{2p}. \end{aligned} \quad (3.15)$$

The overlap matrices read

$$\begin{aligned} S_{AB}(\vec{k}) &= S_{Ba}^*(\vec{k}) \\ &= \frac{1}{N} \sum_{st} e^{i\vec{k}\cdot(\vec{R}_{sB}-\vec{R}_{tA})} \langle \psi(\vec{r}) | \psi(\vec{r} - (\vec{R}_{sB} - \vec{R}_{tA})) \rangle \\ &= s_0 f(\vec{k}) \end{aligned} \quad (3.16)$$

with  $s_0 = \langle \psi(\vec{r}) | \psi(\vec{r} + \vec{b}_l^A) \rangle, l = 1, 2, 3$  the overlap integral. Hence

$$\begin{aligned} S_{AA}(\vec{k}) &= S_{BB}(\vec{k}) = \frac{1}{N} \sum_{st} e^{i\vec{k}\cdot(\vec{R}_{sA}-\vec{R}_{tA})} \langle \psi(\vec{r}) | \psi(\vec{r} - (\vec{R}_{sA} - \vec{R}_{tA})) \rangle \\ &= \langle \psi(\vec{r}) | \psi(\vec{r}) \rangle \\ &= 1. \end{aligned} \quad (3.17)$$

Using the following shorthand notation

$$E_0 = H_{AA}S_{AA}, \quad E_1 = S_{AB}H_{AB}^* + H_{AB}S_{AB}^*, \quad (3.18)$$

$$E_2 = H_{AA}^2 - H_{AB}H_{AB}^*, \quad E_3 = S_{AA}^2 - S_{AB}S_{AB}^*, \quad (3.19)$$

the solution of the secular equation is given by

$$E_j(\vec{k}) = \frac{-(-2E_0 + E_1) \pm \sqrt{(-2E_0 + E_1)^2 - 4E_2E_3}}{2E_3}. \quad (3.20)$$

This can be rewritten in

$$E_j(\vec{k}) = \frac{\epsilon_{2p} \pm \gamma_0 |f(\vec{k})|}{1 \pm s_0 |f(\vec{k})|}, \quad j = v, c \quad (3.21)$$

$$|f(\vec{k})| = \sqrt{3 + 2 \cos(k_y a) + 4 \cos\left(\frac{k_y a}{2}\right) \cos\left(\frac{\sqrt{3} k_x a}{2}\right)}. \quad (3.22)$$

The three parameters  $\epsilon_{2p}$ ,  $\gamma_0$  and  $s_0$  are determined empirically. Using the eigenenergies the corresponding normalized eigenvectors can be calculated

$$v(\vec{k}) = (C_{vA}, C_{vB}) = \frac{1}{\sqrt{2}} \left( -\frac{f(\vec{k})}{|f(\vec{k})|}, 1 \right) \quad (3.23)$$

$$c(\vec{k}) = (C_{cA}, C_{cB}) = \frac{1}{\sqrt{2}} \left( \frac{f(\vec{k})}{|f(\vec{k})|}, 1 \right). \quad (3.24)$$

### 3.1.2 Electronic structure of carbon nanotubes

The chiral vector of a nanotube (see figure 3.1) is given by

$$\begin{aligned} \vec{C} &= n\vec{a}_1 + m\vec{a}_2 \\ &\equiv (n, m). \end{aligned} \quad (3.25)$$

Here

$$\vec{a}_1 = \left( \frac{\sqrt{3}}{2}, \frac{1}{2} \right) a \quad \vec{a}_2 = \left( \frac{\sqrt{3}}{2}, -\frac{1}{2} \right) a \quad a = |\vec{a}_1| = |\vec{a}_2| = 2.46 \text{ \AA} \quad (3.26)$$

are the real space translational vectors of graphene and  $n$  and  $m$  are integers which define a particular tube.  $(n, 0)$  are called zigzag,  $(n, n)$  are called armchair and  $(n, m)$  are called chiral tubes. The diameter of a tube is given

by

$$d_t = \frac{L}{\pi} \quad (3.27)$$

where

$$\begin{aligned} L &= |\vec{C}| \\ &= a\sqrt{n^2 + m^2 + nm} \end{aligned} \quad (3.28)$$

is the circumferential length of the carbon nanotube. The chiral angle  $\theta$  is defined as the angle between  $\vec{C}$  and  $\vec{a}_1$

$$\begin{aligned} \cos(\theta) &= \frac{\vec{C} \cdot \vec{a}_1}{|\vec{C}||\vec{a}_1|} \\ &= \frac{2n + m}{2\sqrt{n^2 + m^2 + nm}}. \end{aligned} \quad (3.29)$$

The translational vector  $\vec{T}$  is parallel to the nanotube axis and normal to the chiral vector. It is the unit vector of a 1D carbon nanotube

$$\begin{aligned} \vec{T} &= t_1\vec{a}_1 + t_2\vec{a}_2 \\ &\equiv (t_1, t_2). \end{aligned} \quad (3.30)$$

$t_1$  and  $t_2$  are given by

$$t_1 = \frac{2n + m}{d_R}, \quad t_2 = -\frac{2m + n}{d_R}. \quad (3.31)$$

Here  $d_R$  is the greatest common divisor of  $(2n + m)$  and  $(2m + n)$ . Its length is found by

$$T = |\vec{T}| = \frac{\sqrt{3}L}{d_R}. \quad (3.32)$$

The number of hexagons per unit cell is given by

$$N = \frac{|\vec{C} \times \vec{T}|}{|\vec{a}_1 \times \vec{a}_2|} = \frac{2(n^2 + m^2 + nm)}{d_R} = \frac{2L^2}{a^2 d_R}. \quad (3.33)$$

There are  $2N$  carbon atoms in each unit cell of a single wall carbon nanotube. Using  $\vec{R}_i \cdot \vec{K}_j = 2\pi\delta_{ij}$  we can introduce the reciprocal lattice vectors of the nanotube

$$\vec{K}_1 = c_1\vec{b}_1 + c_2\vec{b}_2 \quad (3.34)$$

$$\vec{K}_3 = c_3\vec{b}_1 + c_4\vec{b}_2. \quad (3.35)$$

Calculating

$$\vec{C} \cdot \vec{K}_1 = 2\pi, \quad \vec{T} \cdot \vec{K}_1 = 0, \quad (3.36)$$

$$\vec{C} \cdot \vec{K}_2 = 0, \quad \vec{T} \cdot \vec{K}_2 = 2\pi. \quad (3.37)$$

we find:

$$c_1 = -\frac{t_2}{N}, \quad c_2 = \frac{t_1}{N} \quad (3.38)$$

$$c_3 = \frac{m}{N}, \quad c_4 = -\frac{n}{N}. \quad (3.39)$$

Hence the reciprocal lattice vectors are given by:

$$\vec{K}_1 = \frac{1}{N}(-t_2\vec{b}_1 + t_1\vec{b}_2) \quad (3.40)$$

$$\vec{K}_2 = \frac{1}{N}(m\vec{b}_1 - n\vec{b}_2). \quad (3.41)$$

## Tight binding of carbon nanotubes

The electronic structure of a single wall carbon nanotube tube is given by zone folding the Brillouin zone of graphene

$$E_\mu(\vec{k}) = E_g\left(k\frac{\vec{K}_2}{|\vec{K}_2|} + \mu\vec{K}_1\right), \quad \mu = 0, \dots, N-1, \quad -\frac{\pi}{T} < k < \frac{\pi}{T}. \quad (3.42)$$

This means that the wave vector in the circumferential direction is quantized. If the cutting line passes through a  $K$  point we have a metallic, otherwise a semiconducting carbon nanotube. The condition for a metallic nanotube is

$$YK = \frac{2n+m}{3}\vec{K}_1, \quad (3.43)$$

which means that  $(2n + m)$  has to be a multiple of 3. Taking  $\epsilon_{2p} = s_0 = 0$  and ignoring curvature effects the nonzero Hamiltonian elements are

$$H_{AB}(\vec{k}) = \gamma_0 f(\vec{k}), \quad H_{BA}(\vec{k}) = H_{AB}^*(\vec{k}), \quad (3.44)$$

$$\begin{aligned} f(\vec{k}) &= \sum_{l=1}^3 e^{-i\vec{k} \cdot \vec{b}_l^A} \\ &= e^{-ik_x a / \sqrt{3}} + 2e^{ik_x a / 2\sqrt{3}} \cos(k_y a / 2) \end{aligned} \quad (3.45)$$

$$k_x = K_1 \cos(\alpha) - K_2 \sin(\alpha) \quad (3.46)$$

$$k_y = K_1 \sin(\alpha) + K_2 \cos(\alpha) \quad (3.47)$$

where  $\alpha = \pi/6 - \theta$ . The energy eigenvalues are a function of  $\alpha$ ,  $K_1$  and  $K_2$ .

$$E_{c,v}(\vec{k}) = \pm \gamma |f(\vec{k})| \quad (3.48)$$

$$|f(\vec{k})| = \sqrt{3 + 2 \cos(k_y a) + 4 \cos(k_y a / 2) \cos(\sqrt{3} k_x a / 2)} \quad (3.49)$$

$$K_1^\mu L = 2\pi\mu, \quad \mu = 0, \dots, N-1, \quad (3.50)$$

$$-\pi/T \leq K_2 \leq \pi/T \quad (3.51)$$

For a zigzag carbon nanotube with  $\alpha = \pi/6$  we find

$$k_x = \frac{1}{2}(\sqrt{3}K_1 - K_2) \quad (3.52)$$

$$k_y = \frac{1}{2}(K_1 + \sqrt{3}K_2) \quad (3.53)$$

$$E_{c,v}(k) = \pm \gamma_0 \sqrt{3 + 2 \cos\left(\frac{2\pi\mu}{n}\right) + 4 \cos\left(\frac{\pi\mu}{n}\right) \cos\left(\frac{\sqrt{3}K_2 a}{2}\right)}. \quad (3.54)$$

For a armchair nanotube with  $\alpha = 0$  we find

$$k_x = K_1 \quad (3.55)$$

$$k_y = K_2 \quad (3.56)$$

$$E_{c,v}(k) = \pm \gamma_0 \sqrt{3 + 2 \cos(K_2 a) + 4 \cos\left(\frac{\pi \mu}{n}\right) \cos\left(\frac{K_2 a}{2}\right)} \quad (3.57)$$

For a known band-structure it is possible to calculate the electronic density of states.

### 3.1.3 Electric dipole vector of carbon nanotubes

In this section we mainly follow [Zar08] and [ZP09]. The electric dipole matrix element is given by

$$\vec{d}_{c\vec{k}',v\vec{k}} = -e \langle \Psi_c(\vec{k}', \vec{r}) | \vec{r} | \Psi_v(\vec{k}, \vec{r}) \rangle. \quad (3.58)$$

Here  $v$  and  $c$  label the valence and conducting bands and  $\Psi_{v,c}(\vec{k}, \vec{r})$  are the eigenfunctions of the unperturbed Hamiltonian with the eigenenergies  $E_{v,c}(\vec{k})$ . This can be rewritten in

$$\langle \Psi_c(\vec{k}', \vec{r}) | \vec{r} | \Psi_v(\vec{k}, \vec{r}) \rangle = \frac{1}{E_c(\vec{k}') - E_v(\vec{k})} \langle \Psi_c(\vec{k}', \vec{r}) | [\hat{H}, \vec{r}] | \Psi_v(\vec{k}, \vec{r}) \rangle. \quad (3.59)$$

$\Psi_{v,c}(\vec{k}, \vec{r})$  can be expanded in Bloch functions which, in turn, can be expanded in atomic functions

$$\begin{aligned} \langle \Psi_c(\vec{k}', \vec{r}) | \hat{H} \vec{r} | \Psi_v(\vec{k}, \vec{r}) \rangle &= \sum_{ij} C_{ci}^*(\vec{k}') C_{vj}(\vec{k}) \\ &\times \langle \phi_i(\vec{k}', \vec{r}) | \hat{H} \vec{r} | \phi_j(\vec{k}, \vec{r}) \rangle \\ &= \frac{1}{N} \sum_{ij} C_{ci}^*(\vec{k}') C_{vj}(\vec{k}) \sum_{st} e^{-i\vec{k}' \cdot \vec{R}_{si}} e^{i\vec{k} \cdot \vec{R}_{tj}} \\ &\times \langle \psi(\vec{r} - \vec{R}_{si}) | \hat{H} \vec{r} | \psi(\vec{r} - \vec{R}_{tj}) \rangle \\ &= \frac{1}{N} \sum_{ij} C_{ci}^*(\vec{k}') C_{vj}(\vec{k}) \sum_{st} e^{-i\vec{k}' \cdot \vec{R}_{si}} e^{i\vec{k} \cdot \vec{R}_{tj}} \\ &\times \langle \psi(\vec{r} - \vec{R}_{si}) | \hat{H} | \psi(\vec{r} - \vec{R}_{tj}) \rangle \vec{R}_{tj}. \end{aligned} \quad (3.60)$$

In the last expression we have used that the atomic orbitals are eigenfunctions of the coordinate operators.  $\langle \vec{r} | \hat{H} \rangle$  can be calculated in a similar way. Hence

$$\begin{aligned} \langle \Psi_c(\vec{k}', \vec{r}) | \vec{r} | \Psi_v(\vec{k}, \vec{r}) \rangle &= \frac{1}{E_{cv}(\vec{k}', \vec{k})} \frac{1}{N} \sum_{ij} C_{ci}^*(\vec{k}') C_{vj}(\vec{k}) \sum_{st} e^{-i\vec{k}' \cdot \vec{R}_{si}} e^{i\vec{k} \cdot \vec{R}_{tj}} \\ &\times \langle \psi(\vec{r} - \vec{R}_{si}) | \hat{H} | \psi(\vec{r} - \vec{R}_{tj}) \rangle (\vec{R}_{tj} - \vec{R}_{si}). \end{aligned} \quad (3.61)$$

Here  $E_{cv}(\vec{k}', \vec{k}) = E_c(\vec{k}') - E_v(\vec{k})$ . By changing the variable of integration from  $\vec{r}$  to  $\vec{r}' = \vec{r} - \vec{R}_{si}$  and after that dropping the prime, we obtain

$$\begin{aligned} \langle \Psi_c(\vec{k}', \vec{r}) | \vec{r} | \Psi_v(\vec{k}, \vec{r}) \rangle &= \frac{1}{E_{cv}(\vec{k}', \vec{k})} \frac{1}{N} \sum_{ij} C_{ci}^*(\vec{k}') C_{vj}(\vec{k}) \sum_{st} e^{-i\vec{k}' \cdot \vec{R}_{si}} e^{i\vec{k} \cdot \vec{R}_{tj}} \\ &\times \langle \psi(\vec{r}) | \hat{H} | \psi(\vec{r} - (\vec{R}_{tj} - \vec{R}_{si})) \rangle (\vec{R}_{tj} - \vec{R}_{si}). \end{aligned} \quad (3.62)$$

Considering graphene with two different atoms  $A$  and  $B$  in a unit cell we find

$$\begin{aligned} \langle \Psi_c(\vec{k}', \vec{r}) | \vec{r} | \Psi_v(\vec{k}, \vec{r}) \rangle &= \frac{1}{E_{cv}(\vec{k}', \vec{k})} \frac{1}{N} (C_{cA}^*(\vec{k}') C_{vB}(\vec{k}) \sum_{st} e^{-i\vec{k}' \cdot \vec{R}_{sA}} e^{i\vec{k} \cdot \vec{R}_{tB}} \\ &\times \langle \psi(\vec{r}) | \hat{H} | \psi(\vec{r} - (\vec{R}_{tB} - \vec{R}_{sA})) \rangle (\vec{R}_{tB} - \vec{R}_{sA}) \\ &+ C_{cB}^*(\vec{k}') C_{vA}(\vec{k}) \sum_{st} e^{-i\vec{k}' \cdot \vec{R}_{sB}} e^{i\vec{k} \cdot \vec{R}_{tA}} \\ &\times \langle \psi(\vec{r}) | \hat{H} | \psi(\vec{r} - (\vec{R}_{tA} - \vec{R}_{sB})) \rangle (\vec{R}_{tA} - \vec{R}_{sB})). \end{aligned} \quad (3.63)$$

With  $\vec{R}_{tB} = \vec{R}_{sA} + \vec{b}_l^A$  and  $\vec{R}_{tA} = \vec{R}_{sB} + \vec{b}_l^B$ , where  $\vec{b}_l^A$  and  $\vec{b}_l^B$  ( $l = 1, 2, 3$ ) are the nearest-neighbor carbon atom vectors, and  $|\vec{b}_l^B| = |\vec{b}_l^A| = a/\sqrt{3}$  the bond length, one finds

$$\begin{aligned} \langle \Psi_c(\vec{k}', \vec{r}) | \vec{r} | \Psi_v(\vec{k}, \vec{r}) \rangle &= \frac{1}{E_{cv}(\vec{k}', \vec{k})} \frac{1}{N} (C_{cA}^*(\vec{k}') C_{vB}(\vec{k}) \sum_s \sum_{l=1}^3 e^{-i(\vec{k} - \vec{k}') \cdot \vec{R}_{sA}} e^{i\vec{k} \cdot \vec{b}_l^A} \vec{b}_l^A \\ &\times \langle \psi(\vec{r}) | \hat{H} | \psi(\vec{r} - \vec{b}_l^A) \rangle \\ &+ C_{cB}^*(\vec{k}') C_{vA}(\vec{k}) \sum_s \sum_{l=1}^3 e^{-i(\vec{k} - \vec{k}') \cdot \vec{R}_{sB}} e^{i\vec{k} \cdot \vec{b}_l^B} \vec{b}_l^B \\ &\times \langle \psi(\vec{r}) | \hat{H} | \psi(\vec{r} - \vec{b}_l^B) \rangle). \end{aligned} \quad (3.64)$$

By defining the atomic dipole vectors

$$\vec{v}_A(\vec{k}) = -\sum_{l=1}^3 e^{-i\vec{k}\cdot\vec{b}_l^A} \vec{b}_l^A, \quad \vec{v}_B(\vec{k}) = -\sum_{l=1}^3 e^{-i\vec{k}\cdot\vec{b}_l^B} \vec{b}_l^B \quad (3.65)$$

and replacing  $\vec{b}_l^A$  and  $\vec{b}_l^B$  by  $-\vec{b}_l^A$  and  $-\vec{b}_l^B$  we find the general form of the electric dipole matrix element

$$\begin{aligned} \vec{d}_{c\vec{k}',v\vec{k}} &= \frac{-e\gamma_0}{NE_{cv}(\vec{k}',\vec{k})} (C_{cA}^*(\vec{k}')C_{vB}(\vec{k}) \sum_s e^{i(\vec{k}-\vec{k}')\cdot\vec{R}_{sA}} \vec{v}_A(\vec{k}) \\ &+ C_{cB}^*(\vec{k}')C_{vA}(\vec{k}) \sum_s e^{i(\vec{k}-\vec{k}')\cdot\vec{R}_{sB}} \vec{v}_B(\vec{k})) \end{aligned} \quad (3.66)$$

with  $\gamma_0 = \langle \phi(\vec{r}) | \hat{H} | \phi(\vec{r} + \vec{b}_l^{A,B}) \rangle$ .

### Parallel polarization

For parallel polarization, where the direction of the electric field is along the nanotube axis  $Z$ , all  $A(B)$  atoms have the same  $Z$  component of the atomic dipole vector  $\vec{v}_A, (\vec{v}_B)$

$$d_{c\vec{k}',v\vec{k}}^Z = \frac{-e\gamma_0}{E_{cv}(\vec{k}',\vec{k})} (C_{cA}^*(\vec{k}')C_{vB}(\vec{k})v_A^Z(\vec{k}) + C_{cB}^*(\vec{k}')C_{vA}(\vec{k})v_B^Z(\vec{k}))\delta_{\vec{k}',\vec{k}}. \quad (3.67)$$

Using  $\vec{b}_l = \vec{b}_l^A = -\vec{b}_l^B$  and therefore

$$v_B^Z(\vec{k}) = -v_A^{Z*}(\vec{k}) \quad (3.68)$$

$$v_B^Z(\vec{k}) = -\sum_{l=1}^3 e^{-i\vec{k}\cdot\vec{b}_l} b_l^Z = \frac{1}{i\gamma_0} \frac{d}{dK_2} H_{AB}(\vec{k}) \quad (3.69)$$

we find:

$$d_{c,v}^Z(\vec{k}) = \frac{-e\gamma_0}{\sqrt{3}E_{cv}(\vec{k})} (C_{cA}^*(\vec{k})v_A^Z(\vec{k}) + C_{cA}(\vec{k})v_A^{Z*}(\vec{k})). \quad (3.70)$$

With the Hamiltonian elements one arrives at

$$v_A^Z(k) = \frac{a}{\sqrt{2}} \sin \alpha (e^{-ik_x a/\sqrt{3}} - e^{ik_x a/2\sqrt{3}} \cos(k_y a/2)) + i a e^{ik_x a/2\sqrt{3}} \cos(\alpha) \sin(k_y a/2) \quad (3.71)$$

$$\begin{aligned} C_{cA}^*(k) v_A^Z(k) &= \frac{1}{\sqrt{2}|f(\vec{k})|} \frac{a}{\sqrt{3}} (\sin(\alpha)(1 - e^{i\sqrt{3}k_x a/2} \cos(k_y a/2) \\ &+ 2e^{-i\sqrt{3}k_x a/2} \cos(k_y a/2) - 2\cos(k_y a/2)^2) \\ &+ i\sqrt{3} \cos(\alpha) \sin(k_y a/2) (e^{i\sqrt{3}k_x a/2} + 2\cos(k_y a/2))) \end{aligned} \quad (3.72)$$

Then the electric dipole vector for parallel polarization is found

$$\begin{aligned} d_{c,v}^Z(k) &= \frac{2ea\gamma_0^2}{\sqrt{3}E_{cv}^2(k)} (\sin(\alpha)(\cos k_y a - \cos \frac{\sqrt{3}k_x a}{2} \cos \frac{k_y a}{2}) \\ &+ \sqrt{3} \cos \alpha \sin \frac{k_y a}{2} \sin \frac{\sqrt{3}k_x a}{2}). \end{aligned} \quad (3.73)$$

### Perpendicular polarization

In the case of perpendicular polarization it is useful to work with right and left handed operators  $v_{\pm} = v_x \pm i v_y$

$$v_x^A(\phi_j) = \frac{1}{2} [e^{i\phi_j} v_+^{A_0}(\vec{k}) + e^{-i\phi_j} v_-^{A_0}(\vec{k})] \quad (3.74)$$

$$v_x^A(\phi_j) = \frac{-i}{2} [e^{i\phi_j} v_+^{A_0}(\vec{k}) - e^{-i\phi_j} v_-^{A_0}(\vec{k})] \quad (3.75)$$

$$v_x^A(\phi_j) = \frac{-1}{2} [e^{i\phi_j} v_+^{B_0}(\vec{k}) + e^{-i\phi_j} v_-^{B_0}(\vec{k})] \quad (3.76)$$

$$v_x^A(\phi_j) = \frac{i}{2} [e^{i\phi_j} v_+^{B_0}(\vec{k}) - e^{-i\phi_j} v_-^{B_0}(\vec{k})]. \quad (3.77)$$

Here  $\phi_j = 2\pi j/N$ , ( $j = 0, 1, \dots, N-1$ ) is the phase difference between two  $A$  or two  $B$  sites. With these atomic dipole vectors the  $x$  and  $y$  components

of the electric dipole matrix element are given by

$$\begin{aligned}
 d_{c\vec{k}',v\vec{k}}^X &= \frac{-e\gamma_0\delta_{\vec{K}_2,\vec{K}'_2}}{2E_{cv}(\vec{k}',\vec{k})} [(C_{cA}^*(\vec{k}')C_{vB}(\vec{k})v_+^{A_0}(\vec{k}) \\
 &\quad - C_{cB}^*(\vec{k}')C_{vA}(\vec{k})v_+^{B_0}(\vec{k}))\delta_{\mu'=\mu+1} \\
 &\quad + (C_{cA}^*(\vec{k}')C_{vB}(\vec{k})v_-^{A_0}(\vec{k}) \\
 &\quad - C_{cB}^*(\vec{k}')C_{vA}(\vec{k})v_+^{B_0}(\vec{k}))\delta_{\mu'=\mu-1}], \tag{3.78}
 \end{aligned}$$

$$\begin{aligned}
 d_{c\vec{k}',v\vec{k}}^Y &= \frac{ie\gamma_0\delta_{\vec{K}_2,\vec{K}'_2}}{2E_{cv}(\vec{k}',\vec{k})} [(C_{cA}^*(\vec{k}')C_{vB}(\vec{k})v_+^{A_0}(\vec{k}) \\
 &\quad - C_{cB}^*(\vec{k}')C_{vA}(\vec{k})v_+^{B_0}(\vec{k}))\delta_{\mu'=\mu+1} \\
 &\quad - (C_{cA}^*(\vec{k}')C_{vB}(\vec{k})v_-^{A_0}(\vec{k}) \\
 &\quad - C_{cB}^*(\vec{k}')C_{vA}(\vec{k})v_+^{B_0}(\vec{k}))\delta_{\mu'=\mu-1}]. \tag{3.79}
 \end{aligned}$$

The next step is to find  $v_{\pm}^{A_0}$  and  $v_{\pm}^{B_0}$ . Therefore we have to look at the positions of the A and B atoms of graphene 3.2 and obtain:

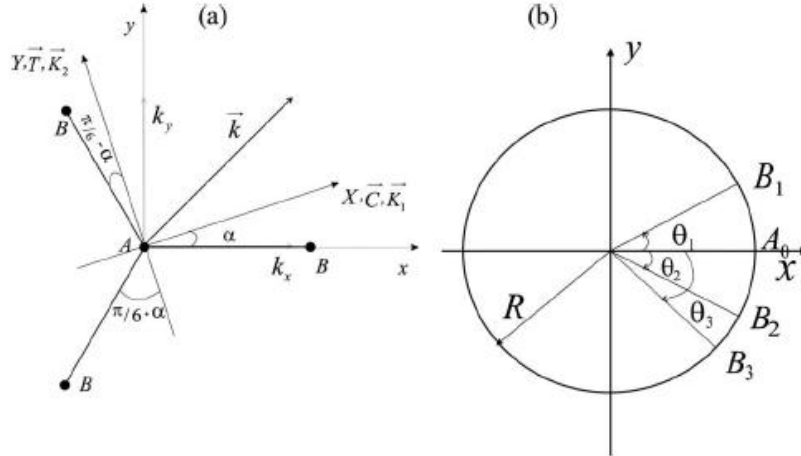


Figure 3.2: Unrolled and rolled-up positions of an A atom and its three nearest B atoms [ZP09].

$$b_{ix}^{A_0} = R \cos(\theta_i) - R, \quad i = 1, 2, 3 \quad (3.80)$$

$$b_{1y}^{A_0} = R \sin(\theta_1), \quad b_{2y}^{A_0} = -R \sin(\theta_2), \quad b_{3y}^{A_0} = -R \sin(\theta_3) \quad (3.81)$$

$$b_{ix}^{B_0} = -b_{ix}^{A_0}, \quad b_{iy}^{B_0} = -b_{iy}^{A_0}. \quad (3.82)$$

Here the angles of the three nearest neighbor atoms are given by

$$\theta_1 = \frac{S_{A_0B_1}}{R} = \frac{\pi(n+m)}{n^2 + m^2 + nm} \quad (3.83)$$

$$\theta_2 = \frac{S_{A_0B_2}}{R} = \frac{\pi m}{n^2 + m^2 + nm} \quad (3.84)$$

$$\theta_3 = \frac{S_{A_0B_3}}{R} = \frac{\pi n}{n^2 + m^2 + nm}. \quad (3.85)$$

For the  $x$  and  $y$  components of atomic dipole vectors we get:

$$\begin{aligned} v_x^{A_0} &= - \sum_{l=1}^3 e^{i\vec{k} \cdot \vec{b}_l^{A_0}} b_{lx}^{A_0} \\ &= -R(e^{-ik_x b} [\cos(\theta_1) - 1] + e^{ik_x b/2 - ik_y b\sqrt{3}/2} [\cos(\theta_2) - 1] \\ &\quad + e^{ik_x b/2 + ik_y b\sqrt{3}/2} (\cos(\theta_3) - 1)) \end{aligned} \quad (3.86)$$

$$\begin{aligned} v_y^{A_0} &= - \sum_{l=1}^3 e^{i\vec{k} \cdot \vec{b}_l^{A_0}} b_{ly}^{A_0} \\ &= R(e^{-ik_x b} \sin(\theta_1) - 1] + e^{ik_x b/2 - ik_y b\sqrt{3}/2} \sin(\theta_2) \\ &\quad + e^{ik_x b/2 + ik_y b\sqrt{3}/2} \sin(\theta_3)) \end{aligned} \quad (3.87)$$

$$v_{x,y}^{B_0} = -v_{x,y}^{A_0*}. \quad (3.88)$$

The right and left handed operators are therefore given by

$$v_{\pm}^{A_0} = v_x^{A_0} \pm i v_y^{A_0} \quad (3.89)$$

$$\begin{aligned}
 v_{\pm}^{A_0} &= R(e^{-ik_x b}(1 - e^{\pm i\theta_1}) + e^{ik_x b/2 - ik_y b\sqrt{3}/2}(1 - e^{\mp i\theta_2}) \\
 &+ e^{ik_x b/2 + ik_y b\sqrt{3}/2}(1 - e^{\mp i\theta_3}))
 \end{aligned} \tag{3.90}$$

$$\begin{aligned}
 v_{\pm}^{B_0} &= -v_{\pm}^{A_0*} = -R(e^{ik_x b}(1 - e^{\mp i\theta_1}) + e^{-ik_x b/2 + ik_y b\sqrt{3}/2}(1 - e^{\pm i\theta_2}) \\
 &+ e^{-ik_x b/2 - ik_y b\sqrt{3}/2}(1 - e^{\pm i\theta_3})).
 \end{aligned} \tag{3.91}$$

They can be rewritten in the following form:

$$v_{\pm}^{A_0} = -v_{\pm}^{B_0*} = |v_{\pm}^{A_0}|e^{i\psi_{\pm}} \tag{3.92}$$

with

$$\psi_{\pm} = \arctan(X_{\pm}/Y_{\pm}) \tag{3.93}$$

$$\begin{aligned}
 X_{\pm} &= -\sin(b_1)[1 - \cos(\theta_1)] \mp \sin(\theta_1) \cos(b_1) \\
 &+ \sum_{i=2}^3 (\sin(b_i)[1 - \cos(\theta_i)] \pm \sin(\theta_i) \cos(b_i))
 \end{aligned} \tag{3.94}$$

$$Y_{\pm} = \sum_{i=1}^3 (\cos(b_i)[1 - \cos(\theta_i)] \mp \sin(\theta_i) \sin(b_i)). \tag{3.95}$$

With the atomic dipole vectors the final form of the electric dipole matrix elements are found:

$$|d_{c\vec{k}',v\vec{k}}^x| = |d_{c\vec{k}',v\vec{k}}^y| = \frac{e\gamma_0 |v_{\pm}^{A_0}| |\delta_{\vec{K}_2\vec{K}'_2}|}{2E_{cv}(\vec{k}', \vec{k})} \left| \sin\left[\frac{2\psi_{\pm}(\vec{k}) - \psi_c(\vec{k}') - \psi_v(\vec{k})}{2}\right] \right| \delta_{\mu'=\mu\pm 1} \tag{3.96}$$

$$\psi_{c,v} = \arctan\left(\frac{2 \cos(k_y b\sqrt{3}/2) \sin(k_x b/2) - \sin(k_x b)}{2 \cos(k_y b\sqrt{3}/2) \cos(k_x b/2) - \cos(k_x b)}\right). \tag{3.97}$$

# Chapter 4

## Imaging excitons in carbon nanotubes with plasmonic nanoparticles

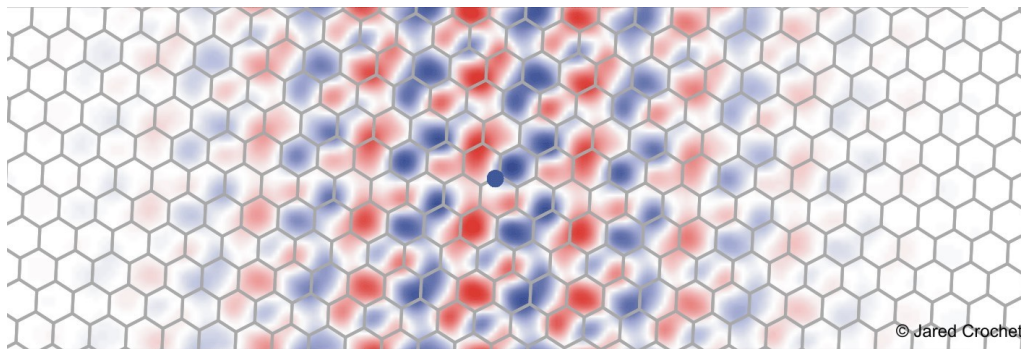


Figure 4.1: In this figure an exciton in a semiconducting single wall carbon nanotube is shown.

### 4.1 Excitons

An exciton can be formed by exciting an electron from the valence band into the conducting band via a photon. In this way a hole in the valence band

is formed to which the electron is bound via the Coulomb force. Excitons describe excitations of the valence electrons in semiconductors. There are two types of limiting cases. If the screening reduces the Coulomb force between the electron and the hole the result is an exciton with a large radius, known as Mott-Wannier exciton. If the Coulomb interaction between the electron and the hole is very strong an exciton with a small radius is formed, which is known as Frenkel exciton.

### 4.1.1 Elementary excitations

An important concept in solid-state physics and nanophysics is the concept of elementary excitations. The main elementary excitations in plasmonics are the plasmons. They are collective excitations which correspond to a collective motion of the system as a whole. Surface plasmon polaritons are normal modes in solids which propagate as electromagnetic waves. The other class of elementary excitations are quasiparticles which correspond to single particles whose motions are modified by interactions with the other particles in the system. Examples are electrons and holes in a solid. The bound state of an electron and a hole via the Coulomb attraction known as exciton is another elementary excitation. For a more detailed discussion of the concept of elementary excitations we refer to [Mad96] and [Mah90].

### 4.1.2 The interband polarization

This section is based on [HK09]. The polarization  $\vec{P}(t)$  is defined as the expectation value of the electric dipole operator  $e\vec{r}$

$$\begin{aligned}\vec{P}(t) &= \sum_s \int d^3r \langle \hat{\Psi}_s^\dagger(\vec{r}, t) e\vec{r} \hat{\Psi}_s(\vec{r}, t) \rangle \\ &= \sum_s \int d^3r \text{tr}[\rho_0 \hat{\Psi}_s^\dagger(\vec{r}, t) e\vec{r} \hat{\Psi}_s(\vec{r}, t)].\end{aligned}\tag{4.1}$$

$\rho_0$  is the equilibrium statistical operator and  $\hat{\Psi}_s^\dagger(\vec{r}, t)$  and  $\hat{\Psi}_s(\vec{r}, t)$  are field operators which are linear combinations of the creation and destruction op-

erators. They are thus operators in the occupation-number Hilbert space

$$\hat{\Psi}(\vec{r}) = \sum_k \Psi_k(\vec{r}) c_k \quad (4.2)$$

$$\hat{\Psi}^\dagger(\vec{r}) = \sum_k \Psi_k(\vec{r})^\dagger c_k^\dagger. \quad (4.3)$$

For spin- $\frac{1}{2}$ -fermions the wave functions have two components

$$\Psi_k(\vec{r}) = \begin{bmatrix} \Psi_k(\vec{r})_1 \\ \Psi_k(\vec{r})_2 \end{bmatrix} = \Psi_k(\vec{r})_\alpha \quad \alpha = 1, 2. \quad (4.4)$$

Field operators fulfill the following commutation and anti-commutation relations for bosons and fermions, respectively:

$$[\hat{\Psi}_\alpha(\vec{r}), \hat{\Psi}_\beta^\dagger(\vec{r}')]_{\mp} = \sum_k \Psi_k(\vec{r})_\alpha \Psi_k(\vec{r}')_\beta^* = \delta_{\alpha\beta} \delta(\vec{r} - \vec{r}') \quad (4.5)$$

$$[\hat{\Psi}_\alpha(\vec{r}), \hat{\Psi}_\beta(\vec{r}')]_{\mp} = [\hat{\Psi}_\alpha^\dagger(\vec{r}), \hat{\Psi}_\beta^\dagger(\vec{r}')]_{\mp} = 0. \quad (4.6)$$

The upper sign refers to bosons and the lower sign refers to fermions. Hamiltonian operators can be written with this operators. These expressions look like the expectation value of a Hamiltonian taken between wave functions, therefore this is often called second quantization. We refer to [Sak67] and [WF03]. In a spatially homogeneous system the field operators can be expanded in a series of Bloch functions  $\Psi_\lambda(\vec{k}, \vec{r})$

$$\hat{\Psi}_s(\vec{r}, t) = \sum_{\lambda, \vec{k}} a_{\lambda, \vec{k}, s}(t) \Psi_\lambda(\vec{k}, \vec{r}). \quad (4.7)$$

Here  $\lambda$  is the band index. Inserting this expansion in the equation of the polarization yields

$$\vec{P}(t) = \sum_{s, \lambda, \lambda', \vec{k}, \vec{k}'} \langle a_{\lambda, \vec{k}, s}^\dagger a_{\lambda', \vec{k}', s} \rangle \int d^3r \Psi_{\lambda, \vec{k}}^*(\vec{r}) e^{i\vec{r} \cdot \vec{k}} \Psi_{\lambda', \vec{k}'}(\vec{r}). \quad (4.8)$$

By calculating the integral

$$\int d^3r \Psi_{\lambda, \vec{k}}(\vec{r}) e \vec{r} \Psi_{\lambda', \vec{k}'}(\vec{r}) \simeq \delta_{\vec{k}, \vec{k}'} \vec{d}_{\lambda \lambda'} \quad (4.9)$$

we obtain the polarization in a spatially homogeneous system

$$\begin{aligned} \vec{P}(t) &= \sum_{\vec{k}, s, \lambda, \lambda'} \langle a_{\lambda, \vec{k}, s}^\dagger(t) a_{\lambda', \vec{k}, s}(t) \rangle \vec{d}_{\lambda \lambda'} \\ &= \sum_{\vec{k}, s, \lambda, \lambda'} P_{\lambda \lambda', \vec{k}, s}(t) \vec{d}_{\lambda \lambda'}. \end{aligned} \quad (4.10)$$

Here

$$P_{\lambda \lambda', \vec{k}, s}(t) = \langle a_{\lambda, \vec{k}, s}^\dagger(t) a_{\lambda', \vec{k}, s}(t) \rangle \quad (4.11)$$

is the pair function. Choosing  $\lambda = v$  and  $\lambda' = c$  and suppressing the spin index  $s$  we find

$$P_{v, c, \vec{k}}(t) = \langle a_{v, \vec{k}}^\dagger(t) a_{c, \vec{k}}(t) \rangle. \quad (4.12)$$

The interaction Hamiltonian between the semiconductor electrons and the electric field is given by

$$H_I = \int d^3r \hat{\Psi}^\dagger(\vec{r}) [-e \vec{r}] \vec{E}(\vec{r}, t) \hat{\Psi}(\vec{r}). \quad (4.13)$$

If the electric field has a monochromatic space dependence

$$\vec{E}(\vec{r}, t) = \vec{E}(t) \frac{1}{2} [e^{i\vec{q} \cdot \vec{r}} + c.c.] \quad (4.14)$$

and assuming a spatially homogeneous system we get

$$H_I \simeq - \sum_{\vec{k}} E(t) (a_{c, \vec{k}}^\dagger a_{v, \vec{k}} d_{cv} + h.c.). \quad (4.15)$$

The Coulomb and kinetic contributions are described by

$$H_{el} = \sum_{\lambda, \vec{k}} E_{\lambda, k} a_{\lambda, \vec{k}}^\dagger a_{\lambda, \vec{k}} + \frac{1}{2} \sum_{\vec{k}, \vec{k}', \vec{q} \neq 0, \lambda, \lambda'} V_q a_{\lambda, \vec{k} + \vec{q}}^\dagger a_{\lambda', \vec{k}' - \vec{q}}^\dagger a_{\lambda', \vec{k}'} a_{\lambda, \vec{k}}. \quad (4.16)$$

For a two-band model we restrict ourselves to  $\lambda, \lambda' = c, v$ .

$$\begin{aligned}
 H_{el} &= \sum_{\vec{k}} [E_{c,k} a_{c,\vec{k}}^\dagger a_{c,\vec{k}} + E_{v,k} a_{v,\vec{k}}^\dagger a_{v,\vec{k}}] \\
 &+ \frac{1}{2} \sum_{\vec{k}, \vec{k}', \vec{q} \neq 0} V_q [a_{c,\vec{k}+\vec{q}}^\dagger a_{c,\vec{k}'-\vec{q}}^\dagger a_{c,\vec{k}} a_{v,\vec{k}} \\
 &+ a_{v,\vec{k}+\vec{q}}^\dagger a_{v,\vec{k}'-\vec{q}}^\dagger a_{v,\vec{k}} a_{c,\vec{k}} + 2a_{c,\vec{k}+\vec{q}}^\dagger a_{v,\vec{k}'-\vec{q}}^\dagger a_{v,\vec{k}} a_{c,\vec{k}}] \quad (4.17)
 \end{aligned}$$

with

$$E_{c,k} = \hbar\epsilon_{c,k} = E_g + \hbar^2 k^2 / 2m_c \quad (4.18)$$

$$E_{v,k} = \hbar\epsilon_{v,k} = \hbar^2 k^2 / 2m_v. \quad (4.19)$$

Here  $m_c$  is the electron mass,  $m_v$  is the hole mass and  $E_g$  is the energy gap. The full Hamiltonian is given by

$$H = H_I + H_{el}. \quad (4.20)$$

The equation of motion for the interband polarization is obtained by inserting it into the Heisenberg equation of motion.

$$\begin{aligned}
 \hbar[i \frac{d}{dt} - (\epsilon_{c,k} - \epsilon_{v,k})] P_{vc,\vec{k}}(t) &= [n_{c,k}(t) - n_{v,\vec{k}}(t)] d_{cv} E(t) \\
 &+ \sum_{\vec{k}', \vec{q} \neq 0} V_q [\langle a_{c,\vec{k}'+\vec{q}}^\dagger a_{v,\vec{k}-\vec{q}}^\dagger a_{c,\vec{k}} a_{c,\vec{k}} \rangle \\
 &+ \langle a_{v,\vec{k}'+\vec{q}}^\dagger a_{v,\vec{k}-\vec{q}}^\dagger a_{v,\vec{k}} a_{c,\vec{k}} \rangle \\
 &+ \langle a_{v,\vec{k}'}^\dagger a_{c,\vec{k}'-\vec{q}}^\dagger a_{c,\vec{k}} a_{c,\vec{k}-\vec{q}} \rangle \\
 &+ \langle a_{v,\vec{k}}^\dagger a_{v,\vec{k}'-\vec{q}}^\dagger a_{v,\vec{k}} a_{c,\vec{k}-\vec{q}} \rangle] \quad (4.21)
 \end{aligned}$$

$$n_{\lambda,\vec{k}} = \langle a_{\lambda,\vec{k}}^\dagger a_{\lambda,\vec{k}} \rangle \quad (4.22)$$

By using the random phase approximation the equation for the interband polarization pair function is found:

$$\hbar\left[i\frac{d}{dt} - (e_{c,k} - e_{v,k})\right]P_{vc,\vec{k}}(t) = [n_{c,\vec{k}}(t) - n_{v,\vec{k}}(t)](d_{cv}E(t) + \sum_{\vec{q}\neq\vec{k}} V_{|\vec{k}-\vec{q}|}P_{vc,\vec{q}}) \quad (4.23)$$

with

$$e_{\lambda,k} = \epsilon_{\lambda,k} + \Sigma_{exc,\lambda}(k) \quad (4.24)$$

$$\hbar\Sigma_{exc,\lambda}(k) = -\sum_{q\neq k} V_{|\vec{k}-\vec{q}|}n_{\lambda,\vec{q}}. \quad (4.25)$$

the renormalized frequencies  $e_{\lambda,k}$  and the exchange self-energy  $\hbar\Sigma_{exc,\lambda}(k)$ .

## Wannier equation

In the situation of quasi-equilibrium and an unexcited crystal we get

$$n_{c,\vec{k}}(t) \rightarrow f_{c,k} \quad \text{and} \quad n_{v,\vec{k}} \rightarrow f_{v,k} \quad (4.26)$$

$$f_{c,k} \equiv 0 \quad \text{and} \quad f_{v,k} \equiv 1. \quad (4.27)$$

The Fourier transform of the equation of motion for the interband polarization is given by

$$(\hbar(\omega + i\delta) - E_g - \frac{\hbar^2 k^2}{2m_r})P_{vc,\vec{k}}(\omega) = -[d_{cv}E(\omega) + \sum_{\vec{q}\neq\vec{k}} V_{|\vec{k}-\vec{q}|}P_{vc,\vec{q}}(\omega)]. \quad (4.28)$$

Here  $1/m_r = 1/m_c - 1/m_v$  is the inverse reduced mass. By multiplying with  $\frac{L^3}{(2\pi)^3} \int d^3k \dots$  from the left and using a Fourier transform  $f(\vec{r}) = \frac{L^3}{(2\pi)^3} \int d^3q f_{\vec{q}} e^{-i\vec{q}\cdot\vec{r}}$  we find:

$$[\hbar(\omega + i\delta) - E_g + \frac{\hbar^2 \vec{\nabla}_r^2}{2m_r} + V(r)]P_{vc}(\vec{r}, \omega) = -d_{cv}E(\omega)\delta(\vec{r})L^3. \quad (4.29)$$

$P_{vc}$  can be expanded into the solution of the corresponding homogeneous equation,

$$\left[\frac{-\hbar^2 \vec{\nabla}_r^2}{2m_r} - V(r)\right]\Psi_\lambda(\vec{r}) = E_v \Psi_\lambda(\vec{r}) \quad (4.30)$$

known as Wannier equation. This equation can be seen as a two-particle Schrödinger equation for the relative motion of a hole and a electron interacting via the attractive Coulomb potential.

## 4.2 The interband polarization for carbon nanotubes

To find the interband polarization for a carbon nanotube we consider the following many-body hamiltonian in the two-band approximation, where we restrict the treatment to one electron and one hole band

$$\begin{aligned} H_0 &= \sum_{i=e,h} \int \psi_i^\dagger(\vec{r}) \left(-\frac{\vec{\nabla}^2}{2m_i} + V_i(\vec{r})\right) \Psi_i(\vec{r}) d\tau \\ &+ \int V_{eh}(\vec{r}, \vec{r}') \Psi_e^\dagger(\vec{r}) \Psi_e(\vec{r}) \Psi_h^\dagger(\vec{r}') \Psi_h(\vec{r}') d\tau d\tau'. \end{aligned} \quad (4.31)$$

Here  $\psi^\dagger(\vec{r})$  and  $\Psi(\vec{r})$  are the field operators. For sufficiently low densities we can ignore  $V_{ee}$  and  $V_{hh}$ . For the optical coupling in rotating wave approximation we have:

$$H_{op} = - \int (\Omega(\vec{r}, t) \Psi_e^\dagger(\vec{r}) \Psi_h^\dagger(\vec{r}) + \Omega^*(\vec{r}, t) \Psi_h(\vec{r}) \Psi_e(\vec{r})) d\tau \quad (4.32)$$

with

$$\Omega = \vec{d} \cdot \vec{E}(\vec{r}, t) \quad (4.33)$$

the Rabi energy. We refer to [IY99] [MW95] [SZ97]. In the rotating wave approximation the terms which oscillate rapidly were neglected. To derive the equation of motion for the interband polarization

$$\vec{d}p(\vec{r}, \vec{r}), \quad (4.34)$$

with the pair function

$$p(\vec{r}_e, \vec{r}_h) = \langle \Psi_h(\vec{r}_h) \Psi_e(\vec{r}_e) \rangle, \quad (4.35)$$

and  $d$  the dipole matrix element we use the Heisenberg equation of motion:

$$[\Psi_e(\vec{r}), H_0] = \left(-\frac{\vec{\nabla}^2}{2m_e} + V_e(\vec{r})\right)\Psi_e(\vec{r}) + \int V_{eh}(\vec{r}, \vec{r}') n_h(\vec{r}') \Psi_e(\vec{r}) d\tau' \quad (4.36)$$

$$[\Psi_h(\vec{r}), H_0] = \left(-\frac{\vec{\nabla}^2}{2m_h} + V_h(\vec{r})\right)\Psi_h(\vec{r}) + \int V_{eh}(\vec{r}, \vec{r}') n_e(\vec{r}') \Psi_h(\vec{r}) d\tau' \quad (4.37)$$

$$[\Psi_e(\vec{r}), H_{op}] = -\Omega(\vec{r}, t) \Psi_h^\dagger(\vec{r}) \quad (4.38)$$

$$[\Psi_h(\vec{r}), H_{op}] = \Omega(\vec{r}, t) \Psi_e^\dagger(\vec{r}) \quad (4.39)$$

with  $n_i(\vec{r}') = \langle \Psi_i^\dagger(\vec{r}') \Psi_i(\vec{r}') \rangle$ . Hence, we find for the time evolution of the pair function:

$$\begin{aligned} i\dot{p}(\vec{r}_e, \vec{r}_h) &= \left(-\frac{\vec{\nabla}_e^2}{2m_e} - \frac{\vec{\nabla}_h^2}{2m_h} + V_e(\vec{r}_e) + V_h(\vec{r}_h)\right)p(\vec{r}_e, \vec{r}_h) \\ &+ \int [V_{eh}(\vec{r}_e, \vec{s}) \langle \Psi_h(\vec{r}_h) n_h(\vec{s}) \Psi_e(\vec{r}_e) \rangle \\ &+ V_{eh}(\vec{s}, \vec{r}_h) \langle \Psi_h(\vec{r}_h) n_e(\vec{s}) \Psi_e(\vec{r}_e) \rangle] ds \\ &- \Omega(\vec{r}_e, t) \langle \Psi_h(\vec{r}_h) \Psi_h^\dagger(\vec{r}_e) \rangle + \Omega(\vec{r}_h, t) \langle \Psi_e^\dagger(\vec{r}_h) \Psi_e(\vec{r}_e) \rangle. \end{aligned} \quad (4.40)$$

With

$$\Psi_h(\vec{r}_h) \Psi_h^\dagger(\vec{r}_e) = \delta(\vec{r}_e - \vec{r}_h) - \Psi_h^\dagger(\vec{r}_e) \Psi_h(\vec{r}_h) \quad (4.41)$$

$$[\Psi_h(\vec{r}_h), n_h(\vec{s})] = \delta(\vec{r}_h - \vec{s}) \Psi_h(\vec{r}_h) \quad (4.42)$$

and considering a low density limit we get

$$\begin{aligned} i\dot{p}(\vec{r}_e, \vec{r}_h) &= \left(-\frac{\vec{\nabla}_e^2}{2m_e} - \frac{\vec{\nabla}_h^2}{2m_h} + V_e(\vec{r}_e) + V_h(\vec{r}_h) + V_{eh}(\vec{r}_e, \vec{r}_h)\right)p(\vec{r}_e, \vec{r}_h) \\ &- \delta(\vec{r}_e - \vec{r}_h) \Omega(\vec{r}_e, t). \end{aligned} \quad (4.43)$$

For an exciton without a confinement potential the following equation of motion holds:

$$\left(-\frac{\vec{\nabla}^2}{2\mu} + V_{eh}(\vec{\rho})\right)\phi_0(\vec{\rho}) = \epsilon_0\phi_0(\vec{\rho}). \quad (4.44)$$

Here  $\mu$  is the reduced mass and  $\vec{\rho}$  is relative coordinate. In the rigid-exciton approximation the center-of-mass and the relative coordinates are decoupled

$$p(\vec{r}_e, \vec{r}_h) = P(\vec{r})\phi_0(\vec{\rho}). \quad (4.45)$$

$\vec{r}$  is the center of mass coordinate and  $\vec{\rho}$  the relative coordinate. Hence

$$i\dot{P}(\vec{r})\phi_0(\vec{\rho}) = \left(-\frac{\vec{\nabla}^2}{2M} + V_e(\vec{r}_e) + V_h(\vec{r}_h) + \epsilon_0\right)\phi_0(\vec{\rho})P(\vec{r}) - \delta(\rho)\Omega(\vec{r} + \frac{\vec{\rho}}{2}, t). \quad (4.46)$$

This can be rewritten in

$$i\dot{P}(\vec{r}) = \left(-\frac{\vec{\nabla}^2}{2M} + V(\vec{r})\right)P(\vec{r}) - \phi_0(0)\Omega(\vec{r}, t), \quad (4.47)$$

with

$$V(\vec{r}) = \int (V_e(\vec{r} + \frac{\vec{\rho}}{2}) + V_h(\vec{r} - \frac{\vec{\rho}}{2}) + \epsilon_0)\phi_0^2(\vec{\rho})d\rho \quad (4.48)$$

the center-of-mass potential. We refer to [ZGR97]. The polarization becomes

$$\vec{d}p(\vec{r}, \vec{r}) = \vec{d}\phi_0(0)P(\vec{r}). \quad (4.49)$$

Considering different exciton polarizations  $\lambda$ , with the same exciton wavefunction  $\phi_0$ , and one spatial dimension  $z$  in the direction of the nanotube axis, we have:

$$\vec{P}(z) = \phi_0(0) \sum_{\lambda} \vec{d}_{\lambda} P_{\lambda}(z) \quad (4.50)$$

$$i\dot{P}_{\lambda}(z) = \left(-\frac{\partial_z^2}{2M} + V(z)\right)P_{\lambda}(z) - \Omega_{\lambda}(z, t) \quad (4.51)$$

$$\Omega_{\lambda}(z) = \phi_0(0)\vec{d}_{\lambda}\vec{E}(z, t). \quad (4.52)$$

The interaction with the electromagnetic field is described through a dyadic Green function  $\hat{G} = \hat{G}_0 + \hat{G}_{refl}$ , where  $\hat{G}_0$  is the dyadic Green function of

vacuum and  $\hat{G}_{refl}$  describes the reflection at the metallic nanoparticle. The Green function provides the link between the current source and the electric field. If the electric field depends on the orientation of the source the Green's function must account for all possible orientations and it has to be a tensor. We refer to [Che99]. Hence

$$\Omega_\lambda(z) = \phi_0(0)\vec{d}_\lambda\vec{E}_{inc}(z) + \phi_0^2(0) \int \sum_{\lambda'} \vec{d}_\lambda\hat{G}_{refl}(z, z')\vec{d}_{\lambda'}P_{\lambda'}(z')dz'. \quad (4.53)$$

Here  $\vec{E}_{inc}$  is the incoming field and  $\hat{G}_{refl}$  is the part which is associated with the reflection at the metallic nanoparticle. We find:

$$\begin{aligned} \omega P_\lambda(z) &= \left(-\frac{\partial_z^2}{2M} + V(z)\right)P_\lambda(z) - \vec{d}_\lambda\vec{E}_{inc}(z) \\ &\quad - \sum_{\lambda'} \int \vec{d}_\lambda\hat{G}_{refl}(z, z')\vec{d}_{\lambda'}P_{\lambda'}(z')dz' \end{aligned} \quad (4.54)$$

with

$$\vec{d}_\lambda = \phi_0(0)\vec{d}_\lambda. \quad (4.55)$$

To find the normalization of the wavefunction

$$\phi_0 = xe^{-c}, \quad (4.56)$$

with

$$c = \sqrt{\frac{s^2}{k^2} + \frac{z^2}{k^2}} \simeq \frac{r}{k} \quad (4.57)$$

where  $k$  is a variational parameter used to minimize the energy and is found to be close to 0.5 we calculate

$$x^2 2\pi \int_0^\infty r e^{-4r} dr = x^2 \frac{\pi}{8} \stackrel{!}{=} 1 \quad (4.58)$$

and get

$$x = 2\sqrt{\frac{2}{\pi}} = \sqrt{\frac{8}{\pi}}. \quad (4.59)$$

Hence

$$\phi_0(0) = \sqrt{\frac{8}{\pi}}. \quad (4.60)$$

We refer to [Kam07] and [Ped03]. By solving

$$\begin{aligned} \omega P_\lambda(z) &= \left(-\frac{\partial_z^2}{2M} + V(z)\right)P_\lambda(z) - \vec{d}_\lambda \vec{E}_{inc}(z) \\ &\quad - \sum_{\lambda'} \int \vec{d}_\lambda \hat{G}_{refl}(z, z') \vec{d}_{\lambda'} P_{\lambda'}(z') dz' \end{aligned} \quad (4.61)$$

for  $P_\lambda(z)$  the polarization of the carbon nanotube can be calculated.

## Results

Figure 4.2 shows the first 10 wave functions and the confinement potential of the excitons. Figure 4.3 shows the normalized scattered intensity for  $z$ -polarized light propagating in the  $x$ -direction and exciting a system consisting of a (1,0) zigzag carbon nanotube in  $z$ -direction and a spherical metallic nanoparticle with different  $x$ -positions relative to the nanotube. The diameter of the nanoparticle was chosen 2.5 nm. For gold the dielectric function of [JC72] and for the background the dielectric function of water  $\epsilon_{out} = 1.5^2$  was used. The positions of the metallic nanoparticle which were studied were (10, 0, 0) nm, (10, 0, 100) nm and (10, 0, 150) nm. Here (0, 0, 0) is the center of the nanotube. The energy gap of the carbon nanotube was given by 2.3 eV. The damping of the excitons in the carbon nanotube was given by  $\gamma = 0.1 \cdot 10^{-3}$  eV and the exciton mass was given by  $2 m_e$ . The dipole moment of the excitons along the three spatial directions for the (1,0) zigzag carbon nanotube was given by  $e \cdot \vec{r} = e \cdot [0, 0, 0.142028]$  nm. The resonance energy and amplitude of the scattered intensity of the coupled system shifts for the different positions of the metallic nanoparticle relative to the carbon nanotube.

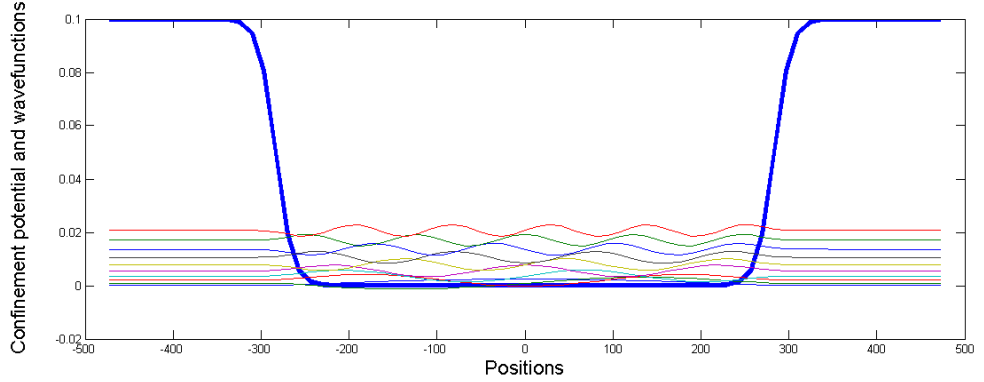


Figure 4.2: This figure shows the first 10 wave functions and the confinement potential of the excitons.

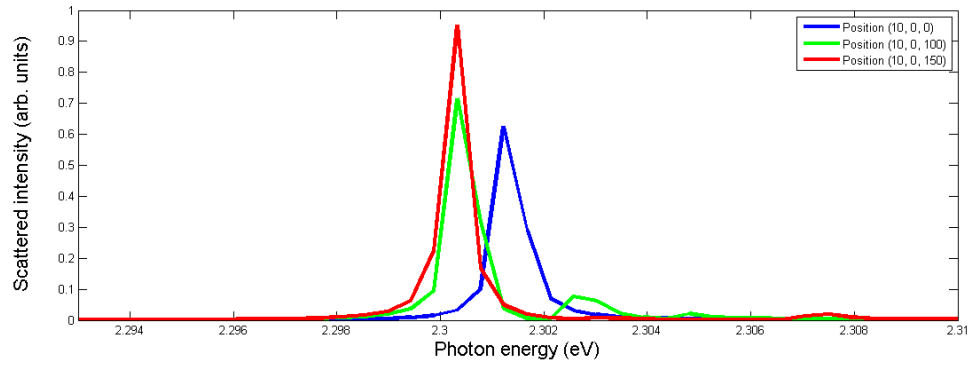


Figure 4.3: Scattered intensity for  $z$ -polarized light propagating in the  $x$ -direction and exciting a system consisting of a  $(1, 0)$  zigzag carbon nanotube in  $z$ -direction and a spherical gold nanoparticle with different  $x$ -positions relative to a the nanotube. The diameter of the nanoparticle was chosen 2.5 nm. The positions of the metallic nanoparticle which were studied were  $(10, 0, 0)$  nm ,  $(10, 0, 100)$  nm and  $(10, 0, 150)$  nm . Here  $(0, 0, 0)$  is the center of the nanotube. For gold the dielectric function of [JC72] and for the background the dielectric function of water  $\epsilon_{out} = 1.5^2$  was used. The energy gap of the carbon nanotube was given by 2.3 eV. The damping of the excitons in the carbon nanotube was given by  $\gamma = 0.1 \cdot 10^{-3}$  eV and the exciton mass was given by  $2 m_e$ . The dipole moment of the excitons along the three spatial directions for the  $(1, 0)$  zigzag carbon nanotube was given by  $e \cdot \vec{r} = e \cdot [0, 0, 0.142028]$  nm .

# Chapter 5

## Conclusion

We studied the imaging of excitons in single-walled carbon nanotubes with plasmonic nanoparticles. We investigated the scattered intensity for different positions of the metallic nanoparticle relative to the carbon nanotube. In particular, we considered a system consisting of a  $(1,0)$  zigzag carbon nanotube coupled to a gold nanoparticle. The same procedure can be used for other types of carbon nanotubes with other parallel and perpendicular electric dipole matrix elements.



# Danksagung

An erster Stelle möchte ich mich bei meiner Mutter **Heidemarie Waxenegger**, meinem Vater **Günther Waxenegger** und meinem Bruder **Günther Waxenegger** bedanken. Ohne Eure Unterstützung wäre das Studium und diese Diplomarbeit unmöglich gewesen.

Mit meinem Betreuer **Ao.Univ.Prof.Mag.Dr. Ulrich Hohenester** hatte ich das Glück von einem großartigen Menschen und Physiker lernen zu dürfen. Vielen Dank.

Desweiteren möchte ich mich bei **Hajreta Softić**, **Andreas Trügler** und den anderen Gruppenmitgliedern für die schönen gemeinsamen Erlebnisse und aufschlussreichen Gespräche bedanken.

Zu guter Letzt möchte ich mich bei allen meinen Freunden und Verwandten welche mich während des Studiums motiviert und unterstützt haben bedanken.



# Bibliography

- [Aus06] H. Aussenegg, F. Ditlbacher. Nanooptik: Plasmonen als lichttransporter. *Physik in unserer Zeit*, 2006.
- [Boy02] Ph. Maali A. Lounis B. Orrit M. Boyer, D. Tamarat. Photothermal imaging of nanometer-sized metal particles among scatterers. *Science*, 2002.
- [CBR07] J. C. Charlier, X. Blase, and S Roche. Electronic and transport properties of nanotubes. *Rev. of. mod. phys.*, 2007.
- [Che99] W. C. Chew. *Waves and Fields in Inhomogenous Media*. IEEE Press, 1999.
- [EQ75] A. Eguiluz and J. J. Quinn. Hydrodynamic model for surface plasmons in metals and degenerate semiconductors. *Phys. Rev. Lett.*, 1975.
- [Fis88] D. W. Fischer, U. Ch. Pohl. Observation of single-particle plasmons by near-field optical microscopy. *Phys. Rev. Lett*, 1988.
- [FM03] D. R. Fredkin and I. D. Mayergoyz. Resonant behavior of dielectric objects (electrostatic resonances). *Phys. Rev. B*, 2003.
- [GH98] F. J. Garcia de Abajo and A. Howie. Relativistic electron energy loss and electron-induced photon emission in inhomogeneous dielectrics. *Phys. Rev. B*, 1998.

- [GH02] F. J. Garcia de Abajo and A. Howie. Retarded field calculation of electron energy loss in inhomogeneous dielectrics. *Phys. Rev. B*, 2002.
- [Har05] H. Meixner A. J. Anderson N. Minami F. Novotny L. Hartschuh, A. Qian. Nanoscale optical imaging of excitons in single-walled carbon nanotubes. *Nano Letters*, 2005.
- [Has02] S. Hassani. *Mathematical Physics*. Springer, 2002.
- [HK05] U. Hohenester and J. Krenn. Surface plasmon resonances of single and coupled metallic nanoparticles: A boundary integral method approach. *Phys. Rev. B*, 2005.
- [HK09] H. Haug and S. W Koch. *Quantum Theory of the Optical and Electronic Properties of Semiconductors*. World Scientific Publishing Company, 2009.
- [HT08a] U. Hohenester and A. Trügler. Interaction of single molecules with metallic nanoparticles. *Phys. Rev. B*, 2008.
- [HT08b] U. Hohenester and A. Trügler. Strong coupling between a metallic nanoparticle and a single molecule. *Phys. Rev. B*, 2008.
- [HW05] H. Haken and H. C. Wolf. *The Physics of Atoms and Quanta: Introduction to Experiments and Theory*. Springer, 2005.
- [Iij91] S. Iijima. Helical microtubules of graphitic carbon. *Nature* 354, 56-58, 1991.
- [IY99] A. Imamoglu and Y. Yamamoto. *Mesoscopic Quantum Optics*. Wiley, 1999.
- [Jac98] J. D. Jackson. *Classic Electrodynamics*. John Wiley Sons, Inc., 1998.
- [JC72] P. B. Johnson and R. W. Christy. Optical constants of the noble metals. *Phys. Rev. B*, 1972.

- [Kal01] M. Mlynek J. Sandoghdar V. Kalkbrenner, T. Ramstein. A single gold particle as a probe for apertureless scanning near-field optical microscopy. *Journal of Microscopy*, 2001.
- [Kam07] D. Kammerlander. Biexciton stability in carbon nanotubes. Master's thesis, KF Graz, 2007.
- [KB07] P. G. Kik and M. L. Brongersma . *Quantum Theory of the Optical and Electronic Properties of Semiconductors Surface Plasmon Nanophotonics*. Springer, 2007.
- [KG08] M. Kroner and S. Biedermann B. Seidl S. Badolato A. Petroff P. M. Zhang W. Barbour R Gerardot B. D. Warburton R. J. Karrai K. Govorov, A. O. Remi. The nonlinear fano effect. *Phys. Rev. Lett.*, 2008.
- [Mad96] O. Madelung. *Solid-State Theory*. Springer, 1996.
- [Mah90] G. Mahan. *Many-Particle Physics*. Plenum, 1990.
- [Mai07] S. A. Maier. *Plasmonics: Fundamentals and Applications*. Springer, 2007.
- [MFZ05] I. D. Mayergoyz, D. R. Fredkin, and Z. Zhang. Electrostatic (plasmon) resonances in nanoparticles. *Phys. Rev. B*, 2005.
- [MW95] L. Mandl and E. Wolf. *Optical coherence and quantum optics*. Cambridge University Press, 1995.
- [MZM02] I. D. Mayergoyz, Z. Zhang, and G. Miano. Analysis of dynamics of excitation and dephasing of plasmon resonance modes in nanoparticles. *Phys. Rev. B*, 2002.
- [NH06] L. Novotny and B. Hecht. *Principles of Nano-Optics*. Cambridge University Press, 2006.
- [Ped03] T. G. Pedersen. Variational approach to excitons in carbon nanotubes. *Phys. Rev. B*, 2003.

- [Pre07] S. A. Vetterling W. T. Flannery B. P. Press , W. H. Teukolsky. *Numerical Recipes*. Cambridge University Press, 2007.
- [Rei03] C. Maultzsch J Reich, S. Thomson. *Carbon Nanotubes*. Wiley, 2003.
- [Sai99] G. Dresselhaus M. S. Saito, R. Dresselhaus. *Physical Properties of Carbon Nanotubes*. Imperial Collage Press, 1999.
- [Sak67] J. J. Sakurai. *Advanced Quantum Mechanics*. Addison Wesley, 1967.
- [Sak03] J. J. Sakurai. *Modern Quantum Mechanics*. Addison Wesley, 2003.
- [Sqa02] I. Hoffmann P. Marquis-Weible F Sqalli, O. Utke. Gold elliptical nanoantennas as probes for near field optical microscopy. *Journal of Applied Physics*, 2002.
- [SZ97] M. O. Scully and M. S. Zubairy. *Quantum Optics*. Cambridge University Press, 1997.
- [Tor09] T. V. Jmerik V. N. Ivanov S. V. Ogawa Y. Minami F. Toropov, A. A. Shubina. Resonant coupling between a gold-nanosphere plasmon and localized excitons in ingan. *Pss*, 2009.
- [Trü07] A. Trügler. Strong coupling between a metallic nanoparticle and a single molecule. Master's thesis, KF Graz, 2007.
- [WF03] J. D. Walecka and A. L. Fetter. *Quantum Theroy of Many-Particle-Systems*. Dover, 2003.
- [Wro02] L. C. Wrobel . *The Boundary Element Method*. Wiley, 2002.
- [Zar08] A. Zarafi. Analytic Study of the Optical, Electro-optical and Magneto-optical Properties of carbon nanotubes, 2008.
- [ZG06] W. Zhang and G. W. Govorov, A. O. Bryant. Semiconductor-metal nanoparticle molecules: Hybrid excitons and the nonlinear fano effect. *Phys. Rev. Lett.*, 2006.

- [ZGR97] R. Zimmermann, F. Große, and E Runge. Excitons in semiconductor nanostructures with disorder. *Pure and Appl. Chem.*, 1997.
- [ZP09] A. Zarifi and T. G. Pedersen. Universal analytic expression of electric-dipole matrix elements for carbon nanotubes. *Phys. Rev. B*, 2009.